Neurobiology of Disease 220 (2026) 107282

Contents lists available at ScienceDirect

Neurobiology of Disease

journal homepage: www.elsevier.com/locate/ynbdi

The role of the kynurenine pathway in the pathophysiology of autism-like phenotype induced by maternal inflammation in male mice

Danielle Santana-Coelho [a,b], Rafael dos Santos de Bessa [c], Rodrigo Neves Romcy-Pereira [c], Miguel A. de la Flor [a,b], Jason C. O'Connor [a,b,*]

[a] Department of Pharmacology, University of Texas Health Science Center at San Antonio, San Antonio, USA
[b] South Texas Veterans Health System, Audie L. Murphy VA Hospital, San Antonio, USA
[c] Federal University of Rio Grande do Norte, Brain Institute, Natal, Brazil

ARTICLE INFO

Keywords:
Maternal immune activation
Kynurenine
Tryptophan
Autism

ABSTRACT

Autism spectrum disorder (ASD) is a neurodevelopmental disorder with core symptoms that may include deficits in communication, social challenges, and repetitive/stereotyped behavior. The etiology of ASD is not well defined, but both genetic and environmental risk factors have been identified. In animal models, prenatal maternal immune activation precipitates the development of a behavioral phenotype resembling ASD, but the mechanisms by which this occurs are not fully understood. Inflammation can upregulate the kynurenine pathway metabolism through the enzyme indoleamine 2,3-dioxygenase-1 (IDO). Increased levels of kynurenines during development can have deleterious consequences leading to behavioral deficits in adulthood. We sought to determine whether the kynurenine pathway plays a pathogenic role in the development of an ASD-like phenotype using a well-characterized mouse model of maternal immune activation (MIA). Multiparous IDO null (IDO−/−) or C57BL/6 J wild-type dams were administered the viral mimetic polynosinic:polycytidylic acid (Poly IC) at gestational day 12.5. A similar immune response to Poly IC occurred in the maternal plasma and placenta of both genotypes, while kynurenine metabolism was only increased in the fetal tissue of WT mice exposed to Poly IC challenge. Interestingly, *N*-methyl-D-aspartate (NMDA) receptor subunit expression was reduced in the fetal brains of male WT, but not IDO−/−, after MIA with Poly IC. Here, we used machine-learning as an advanced method to evaluate ultrasonic vocalizations. Offspring exposed to prenatal MIA exhibited fewer and less complex ultrasonic vocalizations along with diminished social preference; however, MIA-induced repetitive/stereotyped behaviors were only present in WT mice. Taken together, our data indicate that fetal IDO1-dependent kynurenine metabolism mediates distinct components of the MIA-induced ASD-like phenotype in male mice, which may be related to alterations in the expression of NMDAR subunits during neurodevelopment.

1. Introduction

Autism is a neurodevelopmental disorder that affects 1 in every 31 children in the United States with a significantly higher prevalence of diagnoses in males (Center for Disease Control and Prevention, 2025). There is no cure for ASD, and the etiology of the disorder is still not well understood. Even though genetic factors are important in the development of autism, a significant proportion of ASD cases cannot be explained by genetics alone. Therefore, environmental factors have been implicated as important risk factors in the disruption of neurodevelopment (Beversdorf et al., 2018; Bolton et al., 2014; Boulanger-Bertolus et al., 2018; Christensen et al., 2013).

Maternal infection and inflammation during pregnancy represent prominent environmental risk factors to ASD. Prenatal maternal immune responses, triggered by bacterial, viral, or even autoimmune factors are associated with an increased risk of ASD in the offspring (Atladóttir et al., 2010a, 2010b). Consistent with these observations, animal models of early to mid- gestation maternal immune activation (MIA) induced by bacterial or viral infection, precipitate the development of an ASD-like phenotype in the offspring (Liu et al., 2014a; Vuillermot et al., 2017), whereas late gestation MIA disrupts behavioral development in a manner that more closely resembles negative symptoms of schizophrenia (Meehan et al., 2017). For example, administration of the viral mimetic polyiosinic:polycytidylic acid (Poly IC) to mice

* Corresponding author at: 7703 Floyd Curl Drive, San Antonio, TX 78229.
E-mail address: oconnorj@uthscsa.edu (J.C. O'Connor).

https://doi.org/10.1016/j.nbd.2026.107282
Received 22 July 2025; Received in revised form 19 January 2026; Accepted 19 January 2026
Available online 21 January 2026

at day 12.5 of gestation results in altered pre-pulse inhibition, increased marble burying behavior, deficits in social behavior, and decreased isolation-induced ultrasonic vocalizations (Malkova et al., 2012; Smith et al., 2007a; Wu et al., 2017). Nevertheless, the mechanisms by which prenatal MIA causes the development of ASD or ASD-like phenotypes in the offspring have not been entirely determined.

Maternal infection increases the production of cytokines such as interferon-γ (IFN-γ), tumor necrosis factor-α (TNFα), and interleukin-6 (IL-6). Circulating maternal cytokines can act on placental cells or pass through the placental barrier during mid-gestation exposing the fetus to their proinflammatory effects (Dahlgren et al., 2006; Saito and Saito, 2001). In addition, placental cells also express their own toll-like receptors allowing them to respond directly to pathogens originating in the maternal compartment. Maternal proinflammatory cytokines, particularly IL-6, are critical in the development of the ASD-like phenotype in the MIA model of prenatal administration of poly IC (Wu et al., 2017). However, understanding the pathogenic actions of these cytokines at or across the maternal/fetal interface remains incomplete.

Inflammatory challenges can upregulate the kynurenine pathway (Campbell et al., 2014). The kynurenine pathway (KP) is the predominant metabolic pathway by which tryptophan is metabolized. Through indolamine-2,3-dioxygenase (IDO) and tryptophan-2,3-dioxygenase (TDO), tryptophan is metabolized to kynurenine, which can be further metabolized by kynurenine aminotransferase (KAT) or kynurenine-3-hydroxylase (KMO). KAT enzymes produce kynurenic acid (KYNA), and KMO initiates the oxidative metabolic branch of the pathway that produces 3-hydroxykynurenine (3−HK) and, ultimately, quinolinic acid (QUIN). Notably, KYNA and QUIN are both modulators of NMDA receptor activity, acting as an antagonist or agonist of those receptors, respectively (Lehmann et al., 1983; Perkins and Stone, 1982).

Accumulating evidence implicates kynurenine metabolites in the pathophysiology of neurodevelopmental disorders. For example, while increased KYNA levels have been most strongly associated with schizophrenia (Kegel et al., 2014; Kindler et al., 2019) they are also reported in the polygenic BTBR mouse model of ASD-like phenotype (McTighe et al., 2013). Additionally, experimentally increasing KYNA levels during gestation in rodent models results in neurodevelopmental disruption and phenotypic consequences in the offspring such as deficits in fear conditioning (Pershing et al., 2016). Clinically, increased levels of QUIN have been associated with autism in a cross-sectional study of 15 families that have children with autism (Lim et al., 2016), indicating that a dysregulation of the pathway shifting the metabolism toward one of the branches might have a causal role in the development of ASD (Santana-Coelho, 2024).

In this study, we directly tested the hypothesis that IDO1-mediated kynurenine metabolism plays a causal role in the development of the ASD-like phenotype in the poly IC MIA model. We utilized the previously established and validated poly IC model of MIA (Hsiao and Patterson, 2011) in C57BL6/J mice or in mice (C57BL6/J) with a targeted deletion of the IDO (IDO −/−) gene. After MIA with a single injection of poly IC or vehicle, gestation proceeded undisturbed. Behavioral phenotypes associated with autism (communication, sociability, repetitive behavior) were measured in offspring, while molecular and metabolic changes were assessed in the placenta and fetal brain tissue in a subset of MIA pregnancies. Here we report that prenatal MIA results in an ASD-like phenotype, and targeted deletion of IDO1 prevents the upregulation of KP metabolism in the placenta and fetal brain while mitigating some of the MIA-induced phenotypic changes. Collectively, these finding contribute to mechanistically implicate increased KP metabolism as an important pathogenic factor underlying MIA-induced ASD-like behavior.

2. Materials and methods

2.1. Mice

Indoleamine-2,3-dioxygenase-1 homozygous knockout (IDO −/−) mice were obtained from The Jackson Laboratory (Stock #005867 Bar Harbor, ME) and used to establish an in-house breeding colony at University of Texas Health at San Antonio. Background strain matched C57BL/6 J control mice were maintained concurrently in house. All animals were group-housed (2–5 mice per cage) in standard cages within an integrated ventilation caging system. Randomization was conducted at the breeder-cage level where every other breeder cage was assigned to a treatment (Saline or poly IC). Mouse ID was non-identifiable for group to blind personel. The total of 142 mice were used in the study. Food and water were provided *at libitum*. Animals were maintained on a 12:12 h light/dark cycle with lights off at 11:00 pm. Animal care and use were conducted according to the Guide for the Care and Use of Laboratory Animals, eighth edition (NRC) and was approved by the Institutional Animal Care and Use Committee at the University of Texas Health Science Center at San Antonio.

2.2. Maternal immune activation (MIA)

Polyinosinic:polycytidylic acid (poly IC) was used to induced MIA as previously described (Hsiao and Patterson, 2011). Females were checked twice daily for the presence of vaginal plugs after being paired with males of the same genotype. Wild-type dams were paired with wild-type sires, and IDO −/− dams were paired with IDO−/− sires. The presence of a plug represented gestational day 0.5 (GD0.5). Pregnant dams were randomly chosen to be treated with a single dose of poly IC or saline at gestational day 12.5 (GD12.5). Poly IC (P9582, Sigma Aldrich, St Louis, MO, USA) was diluted in sterile 0.9% sodium chloride and intraperitoneally injected into pregnant mice at the dose of 20 mg/kg. Control groups were injected with an equal volume of saline. After treatment, each dam was returned to its cage and left undisturbed until pups were born. All pups were weaned at postnatal day 21 (PD21) and housed with same-sex littermates. Only male offspring were used in the study.

2.3. Behavioral characterization

2.3.1. Ultrasonic vocalization

Isolation-induced ultrasonic vocalizations (USV) were recorded on postnatal day 7 (PD7) (Mosienko et al., 2015). Pups were separated from their dam and littermates for 10 min before the testing. After 10 min of isolation, pups were placed into a sound-attenuating chamber and an ultrasonic microphone (Dodotronic Ultramic 200 K) was used to record the vocalizations for 5 min. Vocalizations were recorded using Seawave Software (CIBRA, Pavia, Italy) at a sampling rate of 200 kHz. Once the mouse was tested, it was returned to its home cage. USV test was performed during the light phase.

USVs were identified from the recordings by calculating the Shannon entropy of the signal. Ultrasonic vocalizations were analyzed and classified by the Software DeepSqueak (Coffey et al., 2019) using unsupervised learning to quantify and classify distinct types of vocalizations emitted by the animals. The shape (or contour) of the USV, duration, and principal frequency were used as the main USV features within an unsupervised machine learning classifier. DeepSqueak also extracted the time of onset, duration, minimum, and maximum frequency, and mean power of the USVs. Using those parameters, the total number of USVs per animal, the principal frequency distribution, USV onset distribution, inter-USV-interval duration and distribution, and the transition probability between USV types were quantified. All USV analyses were performed in MATLAB R2018A (Mathworks). The definitions of USV parameters measured are detailed in Table 1.

Table 1
Definition of USV parameters quantified by DeepSqueak.

USV parameter	Definition
Call Length	Duration of the calls
Principal Frequency	Median frequency contour of the call
Delta Frequency	Difference between the highest and lowest frequency of the contour.
Slope	Slope of the contour. Measurement of the inclination of the call.
Sinuosity	Length of the path between the first and last points on the contour divided by the Euclidean distance between those points.
Mean Power	Average power spectral density of the contour
Tonality	Measurement of the signal to noise ratio. Values are given by (1-geometric mean of the spectrogram)/ arithmetic mean.
Inter-Usv-Interval	Interval between calls

2.3.2. Grooming

Self-grooming behavior was evaluated by an observer blinded to treatment and genotype during the light phase. At 5 weeks of age, mice were placed in a clear plastic beaker (16 cm diameter x 25 cm height) as previously described (Malkova et al., 2012). Mice were habituated in the beaker for 10 min. Following habituation, behavior was observed for 5 min. Grooming behavior was scored as the time that the animals spent licking, touching, scratching, or biting paws, face, body, or tail.

2.3.3. Marble burying

Marble burying behavior was assessed as previously described (Schwartzer et al., 2013a). At six weeks of age, animals were placed in a testing cage with fresh bedding to habituate for 10 min (cage size: 8 × 18.5 × 10, bedding depth 4 cm). After habituation, the mouse was briefly returned to its home cage while 20 marbles were placed in the test cage in a 4 × 5 grid on top of the bedding. The mouse was returned to the testing cage. Following the 10 min of the test the number of buried marbles was counted. The criteria for marbles to be considered buried was that each marble had to be at least 2/3 covered by bedding. Marble burying was performed during the light phase and scored by an observer blinded to the treatment and genotype of the subjects.

2.3.4. Three chamber test

Social behavior was assessed in the three chamber test as described previously (S. E. P. Smith et al., 2007b). Eight-week old mice were tested in a 63 × 41 × 26 cm acrylic box divided into three equal chambers. A 5 × 5 cm opening allowed mice free passage between all chambers. After a 10 min habituation, where mice were able to freely explore the entire three chamber box, the animals were returned to their home cage while the box was cleaned. An unfamiliar (novel conspecific) mouse of the same sex and age was placed under a wire cup inside one of the outer chambers, while in the opposite outer chamber there was an empty wire cage. Mice were placed in the center chamber and allowed to explore freely for 10 min. The movement of the test mouse was video recorded. In a second phase of the test, a new novel conspecific mouse of the same sex and age was placed under the wire cup in one outer chamber, while the mouse that served as the novel conspecific in the first part of the test remained. The locations of the familiar and novel stranger mice were randomly selected. For 10 min, test mice were able to interact with familiar and novel mice, and the time of interaction was recorded. The social preference index was calculated as [$time_{social}$x100/($time_{social}$ + $time_{non\text{-}social}$)] while the novelty preference index was calculated as [$time_{novel}$x100/($time_{familiar}$ + $time_{novel}$)] and represented as %. Videos were scored by an observer blinded to the treatment and genotype of the subjects.

2.3.5. Prepulse inhibition

Acoustic startle response and prepulse inhibition (PPI) tests were conducted in an acoustic chamber (SR-LAB, San Diego Instruments, San Diego, CA) as previously described (Perez et al., 2019). Briefly, mice were placed in a sound-attenuated chamber and allowed to acclimatize to the background noise (65 dB) for 5 min. Startle response was induced by a pulse of 120 dB for 40 ms repeated ten times. Prepulse inhibition was induced using pre-pulses of 69 dB, 73 dB, and 81 dB that lasted 20 ms and were presented 150 ms prior to the startle pulse. Startle response analysis was automated using SR-LAB Analysis Software and measured from 10 to 80 ms after the onset of the startle pulse. PPI was calculated by the researcher as the difference in startle response following the prepulse following the formula: %PPI = [(startle response - prepulse startle response)/prepulse startle response].

2.4. Tissue collection

A satelite cohort of animals was used for the collection of tissues that were used for the analysis of cytokines, kynurenine pathway metabolites, and enzymes. 24 h following saline or poly IC injections, pregnant dams were humanely euthanized. Maternal blood, fetal brain, and placenta were collected. Blood was centrifuged at 4 °C for 10 mins at 1500 x g for separation of plasma. Plasma, placenta, and brain samples were snap frozen in liquid nitrogen. All samples were stored at −80 °C until homogenization.

2.5. Tissue preparation and RT-qPCR

Placenta samples were homogenized in 600 mL of lysis buffer and brain samples were homogenized in 300 mL of lysis buffer from the PureLink RNA Mini Kit (ThermoFisher Scientific, Waltham, MA) using a BeadRuptor (Omni International, Kennesaw, GA) with 1.4-mm zirconium ceramic oxide beads (Omni International) and settings of pulse duration 45 s, pulse number 2 and rest interval 15 s. After centrifugation, the supernatant was removed, and RNA was isolated using the PureLink RNA Mini Kit according to manufacturer instructions. RNA was eluted in 30 ul of RNase free water. RNA concentrations were determined using the Nanodrop spectrophotometer (Thermo Fisher Scientific), and equal concentrations of RNA were used to reverse transcribe cDNA using the High Capacity cDNA reverse transcription kit (Applied Biosystems, Waltham, MA). cDNA was used for RT-qPCR using Taqman primers and probes (ThermoFisher): glyceraldehyde-3-phosphate dehydrogenase (Gapdh Mm99999915, housekeeping control), indoleamine 2,3 dioxygenase (IDO1 Mm00492590), kynurenine aminotransferase (KAT2 Mm00496169_m1), 3-hydroxyanthanilic acid oxygenase (HAAO Mm00517945_m1), glutamate ionotropic receptor NMDA type subunit 1 (NR1 Mm01336435_g1), NMDAr subunit 2 A (NR2A Mm00433802_m1) and NMDArsubunit 2B (NR2B Mm00433820_m1). qPCR was performed using the Bio-Rad CFX 384 system. Data are expressed as fold change relative to WT saline controls using the ΔΔCt method (Schmittgen and Livak, 2008).

2.6. Multiplex

Cytokine/chemokine proteins were measured using Luminex-based bead array according to the manufacturer's instructions (ProcartaPlex Mouse Cytokine/Chemokine, eBioscience; intra-assay CV <5%). Briefly, placenta samples were homogenized in 30× homogenization buffer (20 mm TrisHCl, 150 mm NaCl, 1× Phosphatase/Proteinase inhibitor) at 4 °C using a BeadRuptor (Omni International, Kennesaw, GA). Placenta and plasma samples were centrifuged for 10 min at 4 °C at 14,000 x g. Bradford assay was used to quantify protein content in placenta homogenates, and samples were diluted to contain equal protein concentrations prior to multiplex assay. Targets measured were IL-6, MCP-1, and IP-10. Results are normalized to % of control (WT Saline) to avoid batch variability.

2.7. Liquid chromatography/ mass spectrometry (LCMS)

Brain, placenta, and plasma samples were prepared for LCMS and

analyzed for kynurenine pathway metabolites as previously described (Parrott et al., 2016). Briefly, thawed plasma samples were diluted 5× with 0.2% acetic acid and 1 mM internal standards. Brain and placenta samples were diluted 30× with 0.2% acetic acid and 1 mM internal standards and then homogenized at 4 °C using a BeadRuptor (Omni International, Kennesaw, GA). The supernatant of the placenta, brain samples, and plasma samples were filtered in a centrifuge at 13500 x*g* for 1 h at 4 °C using Amicon Ultra filters tubes (Millipore, Billerica, Ma, USA). After preparation, samples were analyzed on a Q Exactive mass spectrometer (Thermo Fisher Scientific, Waltham, MA) with on-line separation by Dionex UltiMate 3000 HPLC system (Thermo Fisher Scientific, Waltham, MA) in the Mass Spectrometry Core Facility at the University of Texas Health Science Center at San Antonio. Data collected was analyzed using Xcalibur 2.2 software (Thermo Fisher Scientific Waltham, MA) and expressed as μM of metabolite.

2.8. Data analysis

All data were analyzed using GraphPad Prism 8 (San Diego, CA). Kolmogorov-Smirnov test was used to assess the normality of data distribution. Data are represented as mean ± standard deviation (SD) and analyzed by two-way ANOVA with genotype (WT or IDO−/−) and treatment (Saline or poly IC) as the two factors. Startle response was analyzed with a three-way repeated measures ANOVA with genotype (WT or IDO−/−), treatment (Saline or poly IC), and prepulse (baseline, 69db, 73 dB, or 83 dB) as the three factors. When a significant interaction between the factors was identified, Tukey's post hoc test was used to determine the significance of the differences between the means of the different groups. Statistical significance was considered when $p < 0.05$. When only main effects were identified, significance is denoted by symbols outside the field of the graph, while significance notations from post hoc testing is denoted within the field of the graph. To clarify between-group post hoc comparisons, significant differences between WT Saline and other groups are denoted as (+), between WT Poly IC and other groups, are denoted as (#), and between IDO −/− Saline and other groups are denoted as ($). Spurious data were identified in normally distributed data using Chauvenet's outlier test and omitted from analysis and final number of samples is represented in the figure legend (Heisler and O'Connor, 2015). Two-sample Kolmogorov-Smirnov test was used to analyze cumulative distribution of USVs between groups. Pearson's correlation was used to assess the relationship between fetal and maternal immune response and KP metabolism. To mitigate litter effects, offspring from a minimum of 3 distinct dams/litters were included in the analysis. Additionally, a maximum of 3 pups per litter were used for behavioral and metabolic analysis. Detailed summary of statistical power and effect size can be found in Supplementary Table 1. Power was calculate with the G Power software.

3. Results

3.1. Behavioral characterization

3.1.1. Targeted deletion of indoleamine 2,3 dioxygenase-1 mitigates distinct features of MIA-induced ASD-like behavior

To determine if the kynurenine pathway plays a pathogenic role in the development of ASD-like behavioral phenotypes in the MIA model, we performed a battery of behavioral tests to evaluate deficits in communication, repetitive/stereotyped behavior, sociability, and sensory gating. To verify if the dose of Poly IC used in the study was causing significant pup loss, we compared the size of the litters from dams treated with saline with dams treated with Poly IC. Two-Way ANOVA analysis revealed no difference in the litter size between all groups (Supplementary Fig. 1).

3.1.2. Offspring exposed to prenatal Poly IC-induced MIA exhibit disrupted isolation-induced ultrasonic vocalization patterns independent of genotype

At postnatal day 7 (PD7), offspring were isolated from their littermates and dams to record isolation-induced ultrasonic vocalizations. Total number of vocalizations were reduced by MIA in both genotypes (main effect of treatment; $F_{1,27} = 12.74$, $p = 0.001$) (Fig. 1A). To further assess the effects of MIA on the development of communication characteristics, we analyzed several parameters from the USVs emitted by the animals in the study.

Principal frequency distribution showed a bimodal distribution of USVs in all treatments, where most vocalizations occur between either 50–70 kHz or 80–100 kHz in all genotypes and treatments (Fig. 1B-E). Cumulative distribution of USVs' onset along the recordings show differences between most groups. When comparing the USVs' distribution between WT Saline and WT Poly IC, they do not differ considerably during the first 80 s, with both groups emitting less than 20% of the total calls in this interval. Following this period, WT Saline pups concentrate their USVs' emissions in the interval between the 80 and 200 s of the recording while WT Poly IC USV's percentage of vocalization emitted at that time period is lower when compared to WT Saline pups ($p = 0.0049$, Fig. 1F). When comparing the WT Saline group with the IDO−/− Saline group, the WT genotype emissions are more concentrated in the first two-thirds of the recording, with 80% of the total calls, while the IDO−/− genotype has around 60% of the total calls in the same interval ($p = 0.0020$, Fig. 1G). Comparison between IDO−/− offspring with or without poly IC identified that MIA decreased the percentage of calls performed before 200 s of recording ($p = 0.004$, Fig. 1I). MIA offspring from different genotypes show different cumulative distributions. IDO-MIA offspring present most of its calls after 200 s of recordings while WT-MIA emits more vocalizations in the first 150 s ($p = 0.015$, Fig. 1H). Together, these data indicate that the temporal dynamics of isolation-induced vocalization differs between treatments and genotype.

Main effects of treatment were identified for call length ($F_{1,27} = 7.91$, $p = 0.009$, Fig. 1J), delta frequency ($F_{1,27} = 31.87$, $p < 0.0001$, Fig. 1L), slope ($F_{1,26} = 4.97$, $p = 0.035$, Fig. 1M), sinuosity ($F_{1,27} = 23.93$, $p < 0.001$, Fig. 1N) and tonality ($F_{1,27} = 5.33$, $p = 0.029$, Fig. 1P) where these parameters were similarly altered by MIA in both genotypes. An interaction was identified for mean power ($F_{1,25} = 4.30$, $p = 0.048$) and post hoc analysis revealed a mean power increase only in IDO−/− ($p = 0.006$) (Fig. 1O). Principal frequency and inter-usv-interval were not significantly different between groups (Fig. 1K and Q).

Analysis of vocal repertoire identified twelve unique call types. Pattern and sequence analysis of vocalization repertoire syntax show that the prenatal treatment with poly IC caused the repertoire to be less complex and more repetitive (Fig. 2). Transition between distinct syllables is indicated by arrowed line, while an increased transition probability between calls is illustrated in the graph by arrowed lines with thicker warmer colored connecting lines when compared to controls (Fig. 2B and D). WT Poly IC and IDO−/− Poly IC animals performed only 9 or 8 different types of calls, respectively, while WT and IDO−/− controls presented all 12 different types of calls each. Additionally, the predominant call sequences (transition probability >0.3) by all the groups include 4 to 4, 5 to 5, and 9 to 9 repeats, but MIA offspring showed higher probability of 5 to 5 repeats than controls. MIA also increased the transitions between the calls 2–5, 4–7, 5–9 in both genotypes. Also, in IDO−/− MIA offspring presented increased transitions between 5 and 8 and 5–10 in addition to the transitions found to be increased in WT (Fig. 2A-D).

To quantify the differences between the transition repertoire and the transition probabilities between the syllables between the different groups we calculated the transition probability of call types' pairs for the experimental groups. We pooled all USVs emitted by the animals in the respective groups. Calls with >1 s interval between them were not considered as transition. Also, transition probabilities <1% were not included. To visualize the transition probability data we build graphs, where the nodes represent the call types (Fig. 2E), and the edges

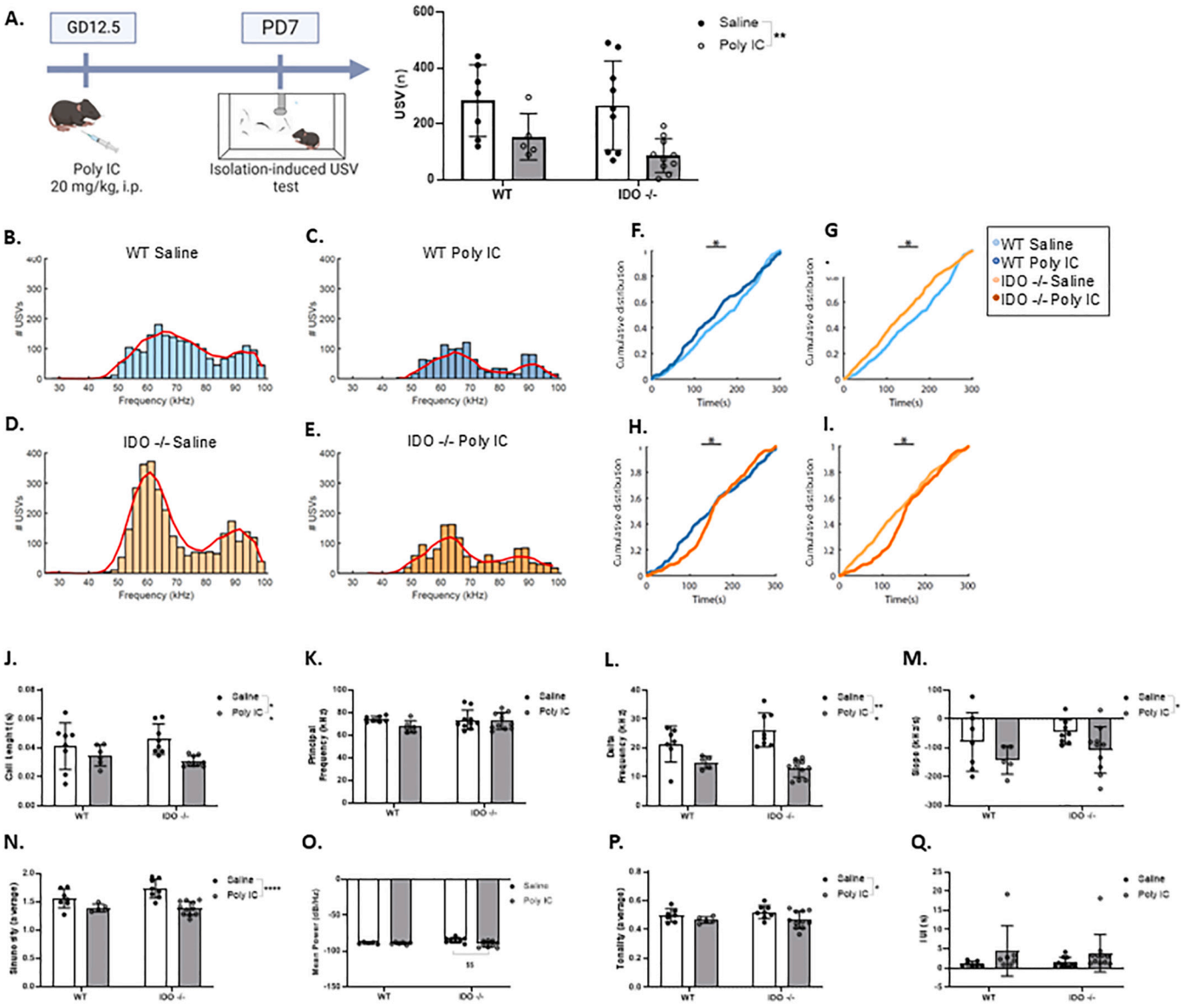

Fig. 1. Ultrasonic vocalization parameters are altered by MIA. A. Pregnant dams were treated with 20 mg/kg of Poly IC at GD12.5 and at PD7 ultrasonic-induced vocalization test was performed. Total number of vocalizations emitted by PD7 offspring when in isolation was decreased by MIA independent of the genotype. B-E. Principal frequency of distribution of USVs showed a bimodal distribution in all groups presenting a concentration of USVs in the 60–70-kHz and 80-100 kHz range. F. Cumulative distribution of USVs' onset along 5 min recordings differed between WT saline vs WT Poly IC (F), WT Saline vs IDO−/− Saline (G), WT Poly IC vs IDO−/− Poly IC (H), IDO −/− Saline vs IDO−/− Poly IC (I). MIA altered call length (J), delta frequency (L), slope (M), sinuosity (N), and tonality (P) independent on the genotype. Mean power was altered by MIA only in IDO−/− offspring (O). Principal frequency and inter-call-interval (IUI) were not altered by MIA (Q). $N = 6–12$. Data are expressed as mean ± SD and Two-Way ANOVA with Tukey Post hoc when appropriate. Cumulative distribution data are analyzed by 2-sample Kolmogorov-Smirnov test. Statistical significance is represented by * < 0.05, ** <. 0.001, and ** $p < 0.001$ $$ < 0.01 vs IDO−/− Saline.

represent the transitions (Fig. 2F). Arrowheads show the direction of the transitions. We build transition graphs for each animal and counted the number of nodes and edges. We did not make a distinction between same-type of edges (circular) and different-type of edges (straight). Animals who emitted <10 USVs were not included in the analysis to avoid bias. Two-way analysis of nodes (call types) demonstrates that there was no effect of treatment or genotype in the total number of different calls performed by the offspring of treated dam independent of the genotype ($p > 0.05$, Fig. 2E). Analysis of transitions (edges) between the syllables, identified a main effect of treatment where poly IC decreased the transitions in both genotypes ($F_{1,31} = 6.41$, $p = 0.04$; Fig. 2F).

3.1.3. *Increased repetitive and stereotyped behavior in MIA offspring is dependent on IDO1*

To evaluate repetitive/stereotyped behavior, self-grooming and marble burying were measured at 5 and 6 weeks of age, respectively. A significant interaction between treatment and genotype ($F_{1,41} = 5.35$, $p = 0.026$) was apparent where poly IC caused an increase in time spent grooming in WT offspring ($p = 0.004$), but not IDO−/− offspring ($p = 0.99$; Fig. 3A). In the marble burying test, a genotype x treatment interaction failed to reach statistical significance ($F_{1,39} = 3.74$, $p = 0.060$) (Fig. 3B). However, due to the trend to significance (p = 0.06) in the interaction, we performed a post hoc analysis and identified that MIA increased marble burying on WT offspring (p = 0.004), but had no effect on IDO −/− offspring ($p = 0.806$, Fig. 3B). Together, these data suggest that the lack of the rate-limiting KP enzyme has a protective effect against the development of repetitive/stereotyped behavior in

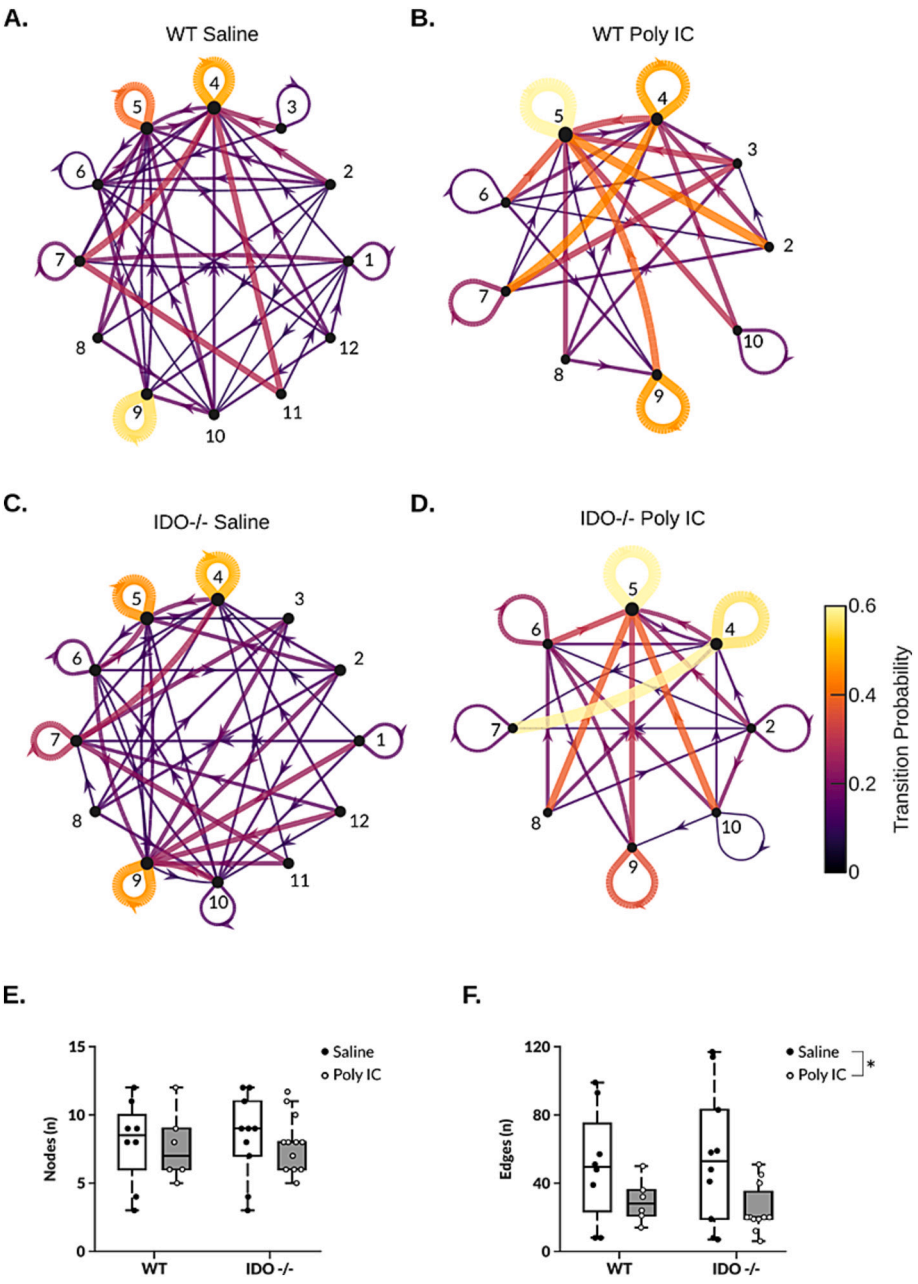

Fig. 2. Vocalization repertoire and syllable transition probability are altered by MIA in both genotypes. A-C. Syntax Path diagrams built with transition probability of USV syllables. Arrows indicate the order of syllable transition between syllables, and thicker lines of warmer color represent higher transition probability. Black dots (nodes) indicate USV call types and bigger dots represent a higher proportion of call types. *E*-F. Quantitative representation of a comparison between the syntax path diagrams. Number of nodes (E) and edges (F), respectively, in individual Syntax Path graphs. Data are expressed as boxplots analyzed with Two-Way ANOVA with Tukey Post hoc. Statistical significance for the main effect of treatment is presented as * $p < 0.05$.

MIA offspring (Fig. 3A and B).

3.1.4. Social behavior deficits in response to prenatal poly IC are not prevented by the lack of IDO

Evaluation of social behavior at eight weeks of age in the three-chamber test revealed that baseline social behavior is similar between WT and IDO−/− mice, where in the sociability part of the test both genotypes spent more time with the mouse than the empty cup (interaction: $F_{1,28} = 0.70$, $p = 0.4086$; genotype: $F_{1,28} = 0.0468$, $p = 0.8304$; target (empty vs mouse_) ($F_{1,28} = 39.98$, $p < 0.0001$; Supplementary Fig. 2A), and in the social novelty part of the test both genotypes spent more time with the novel mouse vs the familiar mouse (interaction: $F_{1,28} = 0.0531$, $p = 0.8193$; genotype: $F_{1,28} = 0.1.608$, $p = 0.2152$; target (familiar mouse vs novel mouse_) ($F_{1,28} = 7.117$, $p = 0.0125$; Supplementary Fig. 2B). Analysis of treatment and genotype identified an effect of MIA on social preference. A main effect of treatment ($F_{1,32} = 16.84$, $p = 0.001$) showed that MIA decreased social preference in both genotypes (Fig. 3C). In the second phase of the test (social novelty), however, the predicted MIA effect of decreasing social novelty preference failed to reach statistical significance ($F_{1,33} = 2.65$, $p = 0.113$) (Fig. 3D). No main effect of genotype or treatment x genotype interaction were apparent in the three-chamber test ($p < 0.05$).

3.1.5. Sensory gating alteration in MIA offspring does not depend on the genotype

Sensory gating deficits were assessed in the prepulse inhibition test

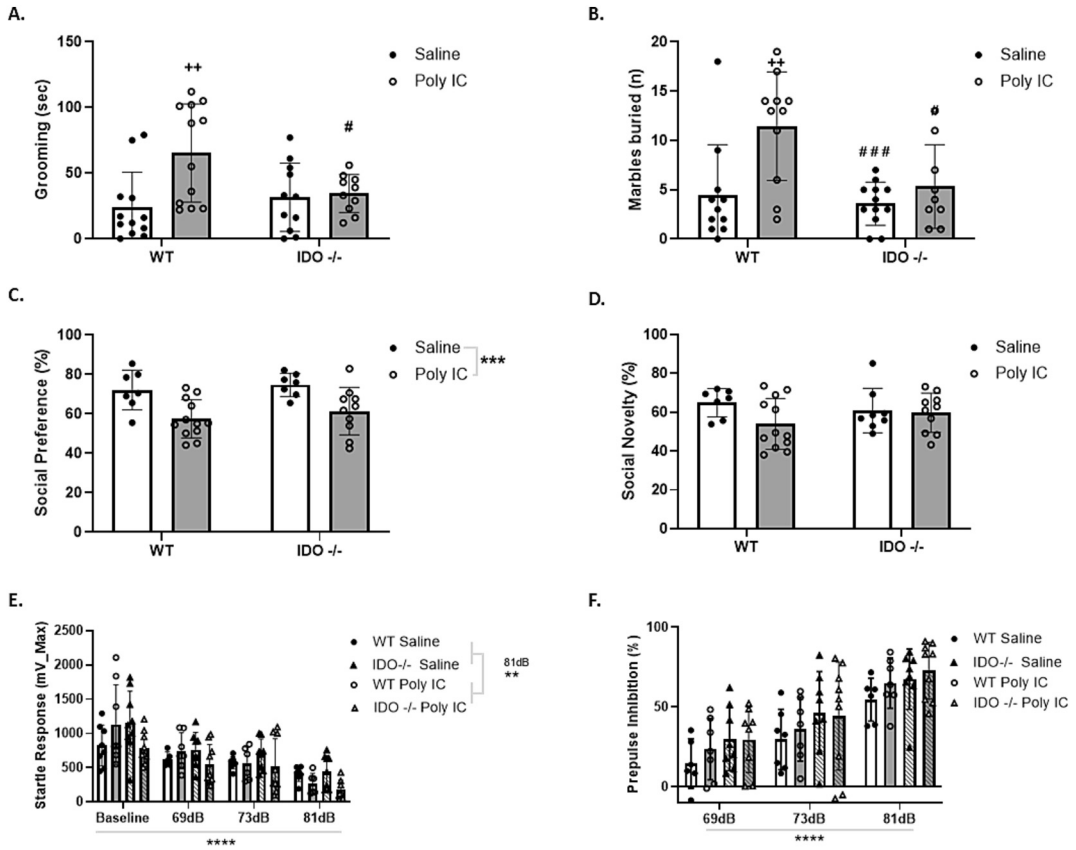

Fig. 3. Lack of IDO is protective against the effects of MIA in repetitive and stereotyped behavior. A-B. Repetitive and stereotyped behavior was evaluated in the grooming and marble burying tests. Total time spent grooming (A) and number of marbles buried (B) were increased by MIA only in WT mice. $N = 9$–12. C-D. Sociability was assessed in the three-chamber test. Social preference was decreased by MIA in both genotypes (C), while social novelty was not affected by prenatal inflammation (D). $N = 6$–12. E. Startle response was measured at baseline and in response to the prepulses of 69 dB, 73 dB and 81 dB. MIA decreased the startle response to the prepulse of 81 dB in both genotypes. F. Percentage of prepulse inhibition was measured with the prepulses of 69 dB, 73 dB and 81 dB. MIA did not alter prepulse inhibition. $N = 5$–9. Data are expressed as mean ± SD analyzed with two-way or three-way ANOVA with Tukey Post hoc. Statistical significance is represented by *** $p < 0.001$.++ $p < 0.01$, and +++ p < 0.001 vs WT Sal. # $p < 0.05$, # # p < 0.01, and # # # p < 0.001 vs WT poly IC.

in 8-week-old mice. A three-way ANOVA revealed a main effect of prepulse ($F_{3,76} = 44.70$, $p < 0.001$) suggesting that the startle response

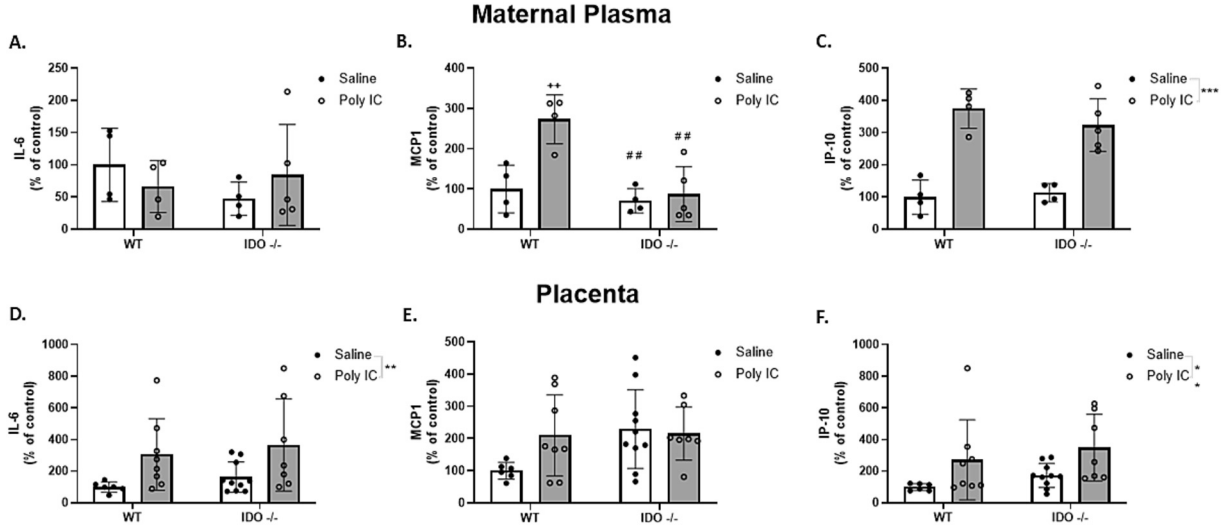

Fig. 4. Immune response 24 h after MIA challenge is distinct in maternal and fetal samples. A-C. Levels of IL-6, MCP1, and IP-10 in maternal plasma 24 h after poly IC administration. MCP1 increased with poly IC administration in WT dams but was not detected in IDO−/− dams 24 h after treatment (B). IP-10 was induced by poly IC in the plasma of dams from both genotypes (C). $N = 4$–5. D-F. Levels of IL-6 (D) and IP10 (F) increased in the placenta 24 h after poly IC administration in both genotypes. MCP1 was not affected by MIA in the placenta (E). $N = 6$–10. Data are expressed as mean ± SD analyzed with Two-Way ANOVA with Tukey Post hoc. Statistical significance is represented by * $p < 0.05$, ** $p < 0.01$ and *** $p < 0.001$. ++ p < 0.01 vs WT sal. # # p < 0.01 vs WT poly IC.

decreased as expected with the increase in the intensity of the prepulse. A two-way interaction between genotype and treatment was identified ($F_{1,31} = 1.49$, $p = 0.043$). Follow up two-way analysis identified a main effect of treatment for the 81 dB startle response indicating that MIA offspring present decreased startle response in both genotypes ($F_{1,26} = 9.99$, $p = 0.004$). Startle responses with a prepulse of 69 dB and 71 dB did not reveal any significant differences between groups. Three-way analysis of prepulse inhibition identified a main effect of prepulse ($F_{1.485,\ 37.11} = 35.43$, $p < 0.0001$) suggesting that as the prepulse increased in intensity the prepulse inhibition decreased in all groups (Fig. 3F).

3.2. Immune and metabolic characterization

3.2.1. MIA-induced immune response differs between maternal and fetal systems

To evaluate maternal and fetal immune response to poly IC treatment, cytokine and chemokine protein levels were measured 24 after poly IC challenge. In maternal plasma, the effect of poly IC on the levels of cytokines and chemokines varied depending on the target that was measured. There were no increase in IL-6 levels at 24 h in any of the groups (Fig. 4A). But, for MCP-1, there was an interaction between genotype and treatment ($F_{1,13} = 7.821$, $p = 0.0151$) where poly IC increased the levels of this chemokine in WT dams ($p = 0.0045$) but not in IDO−/− (Fig. 4B). Last, for IP-10, there was a main effect of treatment ($F_{1,13} = 46.79$, $p < 0.001$) characterized by increased levels of this chemokine in both genotypes (Fig. 4C).

In the placenta, MIA caused a main effect of treatment leading to an increase in the levels of IL-6 ($F_{1,27} = 8.84$, $p = 0.006$) and IP-10 ($F_{1,27} = 7.96$, $p = 0.008$) (Fig. 4D and F). MCP-1 was not affected by MIA in the placenta. No treatment x genotype interactions were apparent in placental tissue following poly IC treatment.

3.2.2. Kynurenine pathway is modulated by MIA in a tissue specific manner

To confirm the activation of KP metabolism during MIA and further investigate the potential role of the kynurenine pathway in mediating the effect of MIA, we measured the expression of KP enzymes and metabolite levels in both maternal and fetal compartments. Maternal levels of kynurenine metabolites were not different 24 h after poly IC injection. However, there was a main effect of genotype, where kynurenine levels were lower in IDO−/− ($F_{1,14} = 16.21$, $p = 0.0013$) when compared to WTs (Fig. 5C).

As expected, in placental homogenates, there was no expression of indoleamine 2,3 dioxygenase 1 (IDO1) in IDO−/− mice. Additionally, MIA had no effect on the expression of IDO1 in WT offspring (Fig. 6A). Two-way ANOVA revealed an interaction between treatment and

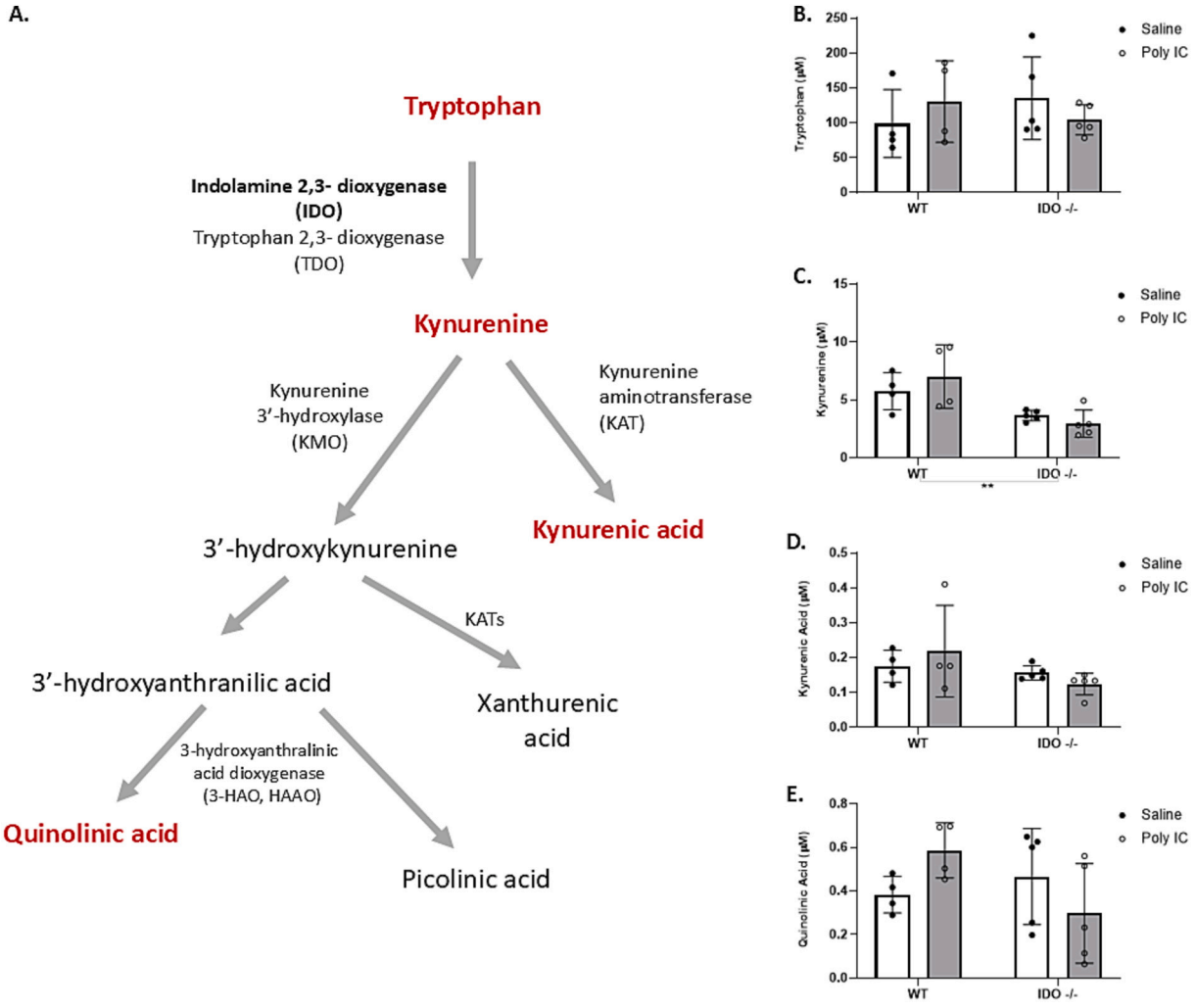

Fig. 5. Maternal kynurenine metabolism is not altered by poly IC 24 h after treatment. A. Kynurenine pathway diagram. B-E. 24 h after maternal Poly IC challenge, levels of kynurenine pathway metabolites were measured in maternal plasma. Levels of kynurenine metabolites were not altered in maternal plasma in response to poly IC treatment. IDO−/− dam's plasma present a lower level of kynurenine than WT dams. N = 4–5. Data are expressed as mean ± SD and analyzed with two-way ANOVA. Statistical significance is represented by ** $p < 0.01$.

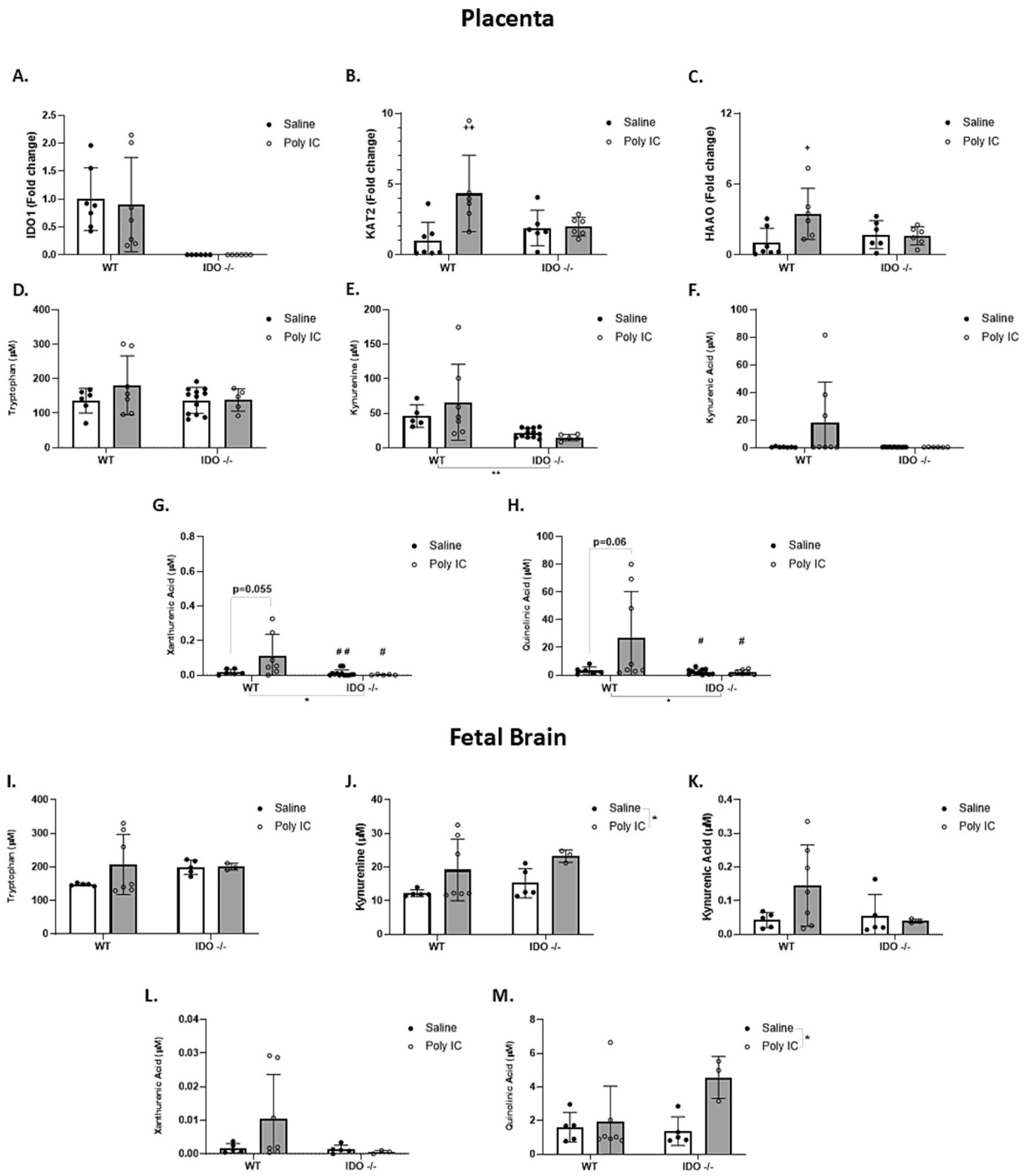

Fig. 6. Kynurenine pathway metabolism is altered in fetal system 24 h after poly IC treatment. 24 h after maternal poly IC challenge, expression of indoleamine 2,3 dioxygenase (IDO), kynurenine transaminase 2 (KAT2), and 3-hydroxyanthranilic acid oxygenase (HAAO) was measured in placental homogenates (A-C), and the levels of kynurenine pathway metabolites were measured in the placenta (D-H) and fetal brain (I-M). MIA upregulated the enzymes KAT2 and HAAO in WT placentas, but did not affect IDO−/− placentas (B and C). N = 6–7. IDO −/− placentas has lower levels of kynurenine (E), xanthurenic acid (G), and quinolinic acid (H) compared to WT placentas. Quinolinic acid (H) and xanthurenic acid were the only metabolites that presented a trend to increased by MIA only in WT placentas, IDO −/− placenta's levels were not altered by poly IC treatment. N = 5–13.MIA increased the levels of kynurenine (J) and quinolinic acid (M) in the fetal brain of both genotypes N = 3–7. Data are expressed as mean ± SD and analyzed with Two-Way ANOVA with Tukey Post hoc. Statistical significance is represented by * $p < 0.05$, and ** $p < 0.01$ + p < 0.05, and ++ p < 0.01 vs WT SAL. # <0.05 and # # <0.01 vs WT Poly IC.

genotype for the expression of kynurenine aminotransferase 2 (KAT2, $F_{1,21} = 6.06$, $p = 0.0226$; Fig. 6B) and 3-hydroxyanthrilic acid dioxygenase (HAAO, $F_{1,21} = 5.05$, $p = 0.0355$; Fig. 6C). Post hoc analysis showed that MIA upregulated the expression of the KP enzymes KAT2 ($p = 0.0051$) and HAAO ($p = 0.0166$) in WT offspring, but the lack of the enzyme in IDO−/− prevented a similar effect to occur (Fig. 6B and C).

Regarding kynurenine metabolites, MIA caused an increase in the mean levels of tryptophan ($p = 0.570$), kynurenine ($p = 0.798$), and kynurenic acid ($p = 0.153$) that did not reach statistical significance in WTs. Quinolinic acid ($F_{1,29} = 4.20$, $p = 0.049$) and xanthurenic acid ($F_{1,27} = 4.98$, $p = 0.034$) were the only metabolites that showed an interaction between genotype and treatment. Post hoc analysis revealed a trend for

quinolinic acid ($p = 0.067$) and xanthurenic acid ($p = 0.055$) to present a difference between MIA and control WT placentas (Fig. 6G and H). MIA had no effect on any of the metabolites measured in IDO−/− mice (Fig. 6H-M). Additionally, a significant main effect of genotype on kynurenine ($F_{1,25} = 11.51$, $p = 0.002$), xanthurenic acid levels ($F_{1,27} = 6.35$, $p = 0.0180$), and quinolinic acid ($F_{1,29} = 4.90$, $p = 0.035$) was apparent with the metabolites being lower in IDO−/− when compared to WT placentas (Fig. 6E, G and H).

Analysis of fetal brain identified a main effect of treatment for kynurenine ($F_{1,16} = 6.88$, $p = 0.018$) and quinolinic acid levels ($F_{1,16} = 6.19$, $p = 0.025$), where in both genotypes there was an increase in the levels of these metabolites (Fig. 6J and M).

3.2.3. Placental IL-6 correlates with fetal kynurenine levels

The correlation between IL-6 levels in the maternal or fetal system with placental kynurenine was quantified to assess whether the cytokine levels are related to the observed upregulation of KP metabolism. Maternal plasma IL-6 levels were not significantly correlated with placental kynurenine levels in either WT or IDO−/− mice 24 h after the treatment (Fig. 7A-B). IL-6 expression in the placenta was significantly correlated ($r = 0.8107$, $p = 0.027$) with kynurenine levels in the placentas of WT offspring (Fig. 7C). For IDO−/−, there was a trend toward a negative correlation ($r = -0.7151$, $p = 0.071$), where higher levels of IL-6 tend to correlate with lower levels of kynurenine (Fig. 7D).

3.2.4. MIA did not alter serotonin metabolism in maternal or fetal sample 24 h after immune stimulation

To assess if MIA could be altering tryptophan metabolism through serotonergic pathway (Fig. 8A), we measured the levels of serotonin (5-HT) and its metabolite 5-hydroxyindole acetic acid (5-HIAA). Due to variability between the two batches of LCMS runs, the samples were normalized to the percentage of control (WT saline) per batch. 5-HT and 5-HIAA level were not significantly altered 24 h after administration of poly IC in maternal plasma, placenta, or fetal brain (Fig. 8B-G). A main effect of genotype showed that IDO−/− placentas presented lower levels of 5-HT when compared to WT ($F_{1,29} = 17.48$, $p = 0.002$, Fig. 8D).

3.3. NMDA expression

3.3.1. MIA-induced decrease in NMDA receptor subunits is genotype-dependent

To further investigate how dysregulation of the kynurenine pathway could be leading to disruption of brain development, we measured the expression of NMDA receptor subunits NR1, NR2A, and NR2B. Two-way ANOVA revealed an interaction between genotype and treatment for NR1 ($F_{1,26} = 8.65$, $p = 0.007$) and NR2B ($F_{1,26} = 4.64$, $p = 0.041$) expression. Post hoc test showed that MIA downregulated the expression of NR1 ($p = 0.0314$) and NR2B ($p = 0.0375$) in WT offspring brains (Fig. 9A and C). In IDO−/− saline, there was a lower expression of all the subunits at baseline when compared to WT saline controls (NR1 $p = 0.008$ and NR2B $p = 0.032$). Additionally, no significant effect of poly IC was identified in IDO−/− for any of the targets measured. A main effect of genotype identified a lower expression of the subunits in knockout brains (NR1 $F_{1,26} = 6.70$, $p = 0.016$; NR2A $F_{1,26} = 4.50$, $p = 0.043$; NR2B $F_{1,26} = 11.18$, $p = 0.002$; Fig. 9A-C).

4. Discussion

Neurodevelopmental disorders such as autism spectrum disorder are associated with prenatal immune challenges, yet the biological pathways that translate maternal inflammation into long-lasting behavioral outcomes remain incompletely understood. The present study identifies kynurenine pathway (KP) metabolism as a potentially clinically relevant mediator of specific behavioral consequences of maternal immune activation (MIA) and potentially other insults that upregulate IDO. Using a well-validated prenatal poly IC model, we demonstrate that genetic deletion of the rate-limiting KP enzyme indoleamine 2,3-dioxygenase 1 (IDO1) selectively prevents the development of repetitive and stereotyped behaviors, while deficits in communication, sociability, and sensory gating persist (Fig. 10). These findings suggest that IDO1-

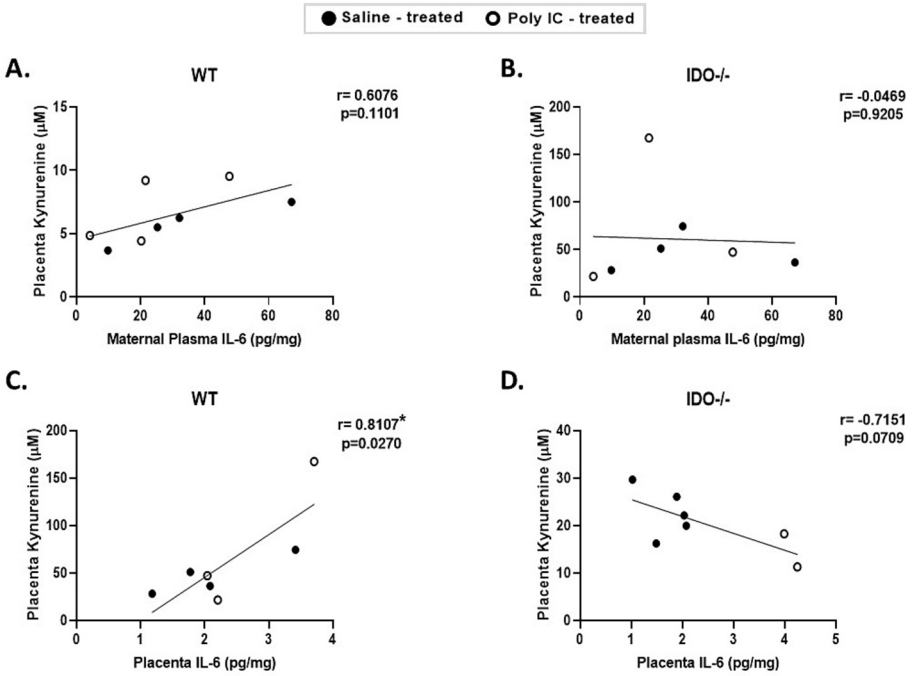

Fig. 7. Relationship between fetal IL-6 and kynurenine levels is dependent on genotype. A-B. Correlation between maternal plasma IL-6 levels and placental kynurenine levels in WT and IDO −/− offspring demonstrate no relationship between the levels of IL-6 in dams and kynurenine in the placenta. C-D. Correlation between placental IL-6 levels and kynurenine levels in WT and IDO−/− offspring. A positive correlation between placental IL-6 and kynurenine levels were identified in WT placenta (C). IDO−/− placentas presented a trend to a negative correlation (D). Data was analyzed using Pearson's Correlation. Statistical significance is represented by * $p < 0.05$.

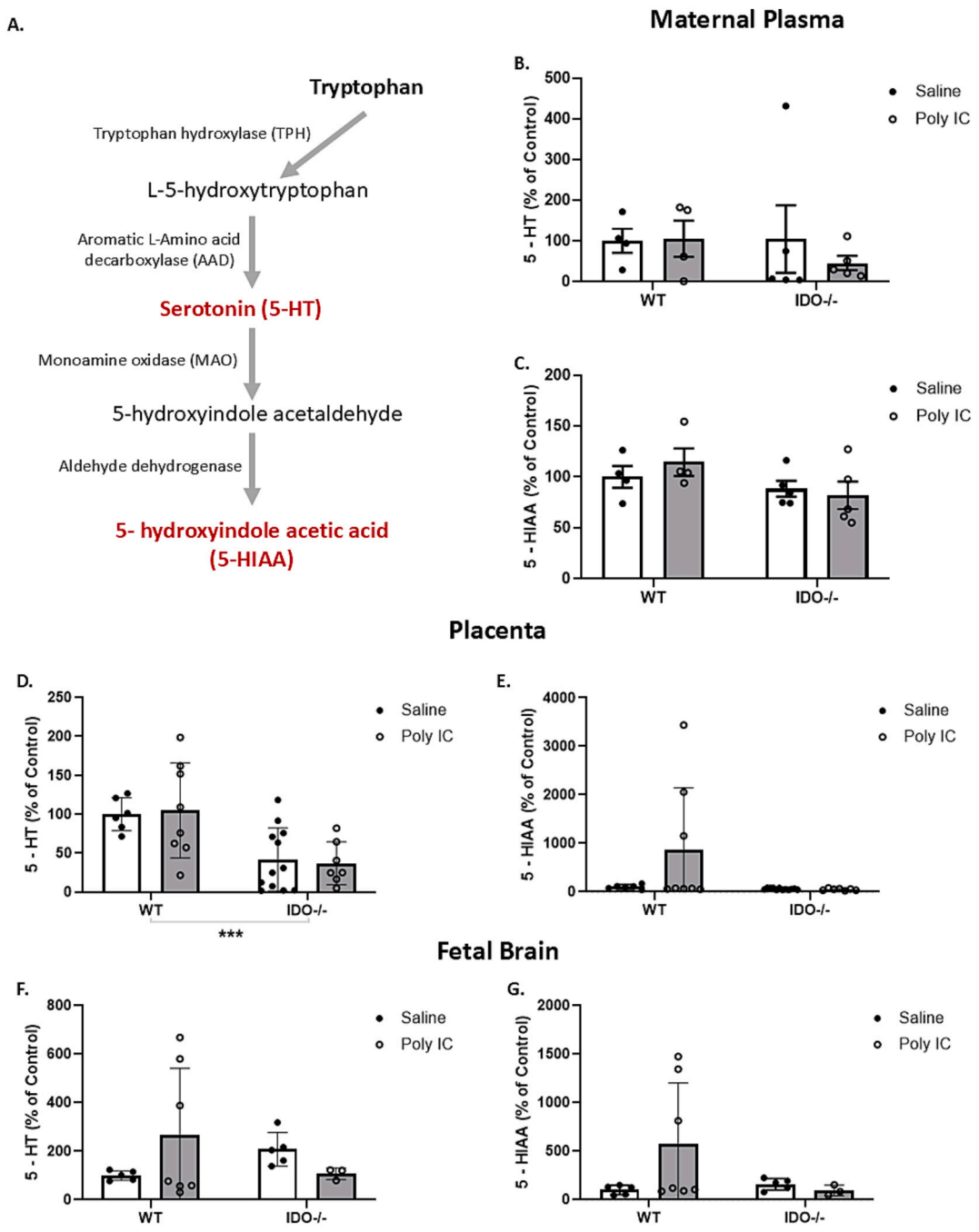

Fig. 8. Levels of 5-HT and 5-HIAA are not altered by MIA at the 24 h timepoint. A. Diagram of serotonin metabolic pathway. 24 h after maternal poly IC challenge, levels of 5-HT and 5-HIAA were measured in the maternal plasma (B-C, $N = 4$–5), placenta (D-E, $N = 6$–12), and fetal brain (F-G, N = 3–7). Poly IC treatment did not alter the levels of 5-HT and 5-HIAA in maternal or fetal samples. 5-HT levels were lower in the placenta of IDO−/− offspring (D). Data are expressed as mean ± SD and analyzed with Two-Way ANOVA. Statistical significance is represented by *** $p < 0.001$.

dependent KP metabolism mechanistically contributes to discrete ASD-like phenotypes, potentially through alterations in neuroactive kynurenine metabolites that influence neuroinflammation and glutamatergic neurotransmission during critical periods of gestation. However, interpretation of these findings is limited by the use of a single MIA model and gestational time point, as well as the absence of direct manipulation of individual KP metabolites, highlighting important directions for future translational studies.

IDO knockout mice have been shown to be protected against the consequences of inflammatory insults. In the LPS sepsis and bacterial peritonitis model, IDO knockout mice exhibit increased survival rates, decreased blood bacterial load, and increased levels of the chemokines MIP-2a and GROα, which are accompanied by recruitment of mononuclear cells and neutrophils to the site of infection (Hoshi et al., 2014). Additionally, we have previously demonstrated that IDO-dependent KP metabolism mediated the depressive-like behavioral consequences of the peripheral immune challenges with either LPS (Salazar et al., 2012) or BCG (O'Connor et al., 2009) in adult mice. IDO−/− mice were also protected from the depressive-like behavioral consequences of direct intracerebroventricular administration of LPS (Lawson et al., 2013). However, to our knowledge, this is the first time that the targeted deletion of IDO has been implicated in the pathogenesis of poly IC maternal immune activation-induced neurodevelopmental disruption.

A variety of maternal immune activation models in rodents have

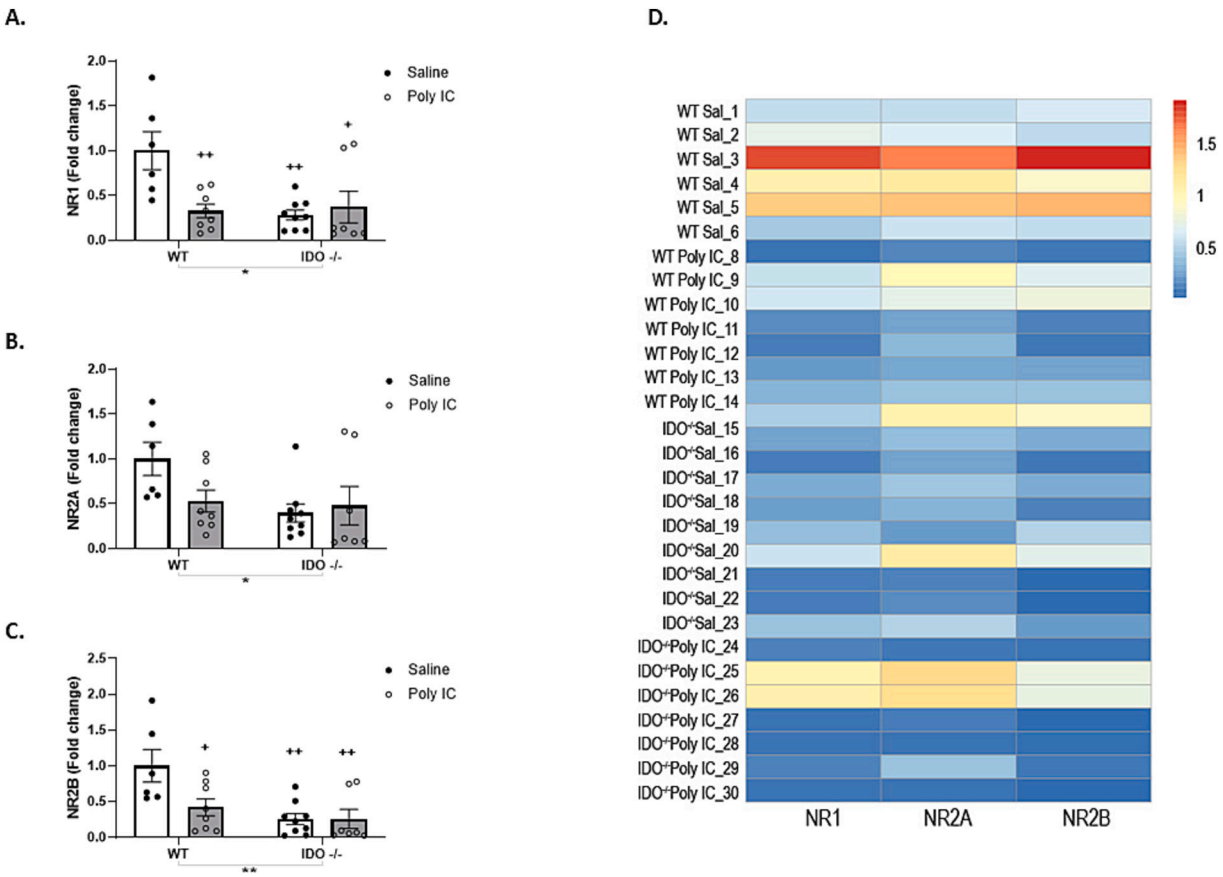

Fig. 9. Fetal brain expression of NMDAr subunits is decreased by poly IC only in WT mice. Expression of NMDA receptor subunits NR1 (A), NR2A (B), NR2B (C) was measured in fetal whole brain 24 h after Poly IC administration to pregnant dams. Poly IC administration decreased the expression of NR1 and NR2B in WT brains. IDO−/− brains presented decreased expression of all subunits measured when compared to WT brains. (D) Heatmap representing fold change of individual samples within each group. N = 6–9. Data are expressed as mean ± SEM and analyzed with Two-Way ANOVA with Tukey Post hoc. Statistical significance is represented by * $p < 0.05$ and ** $p < 0.01$ + $p < 0.05$ and ++ $p < 0.01$ vs WT Sal.

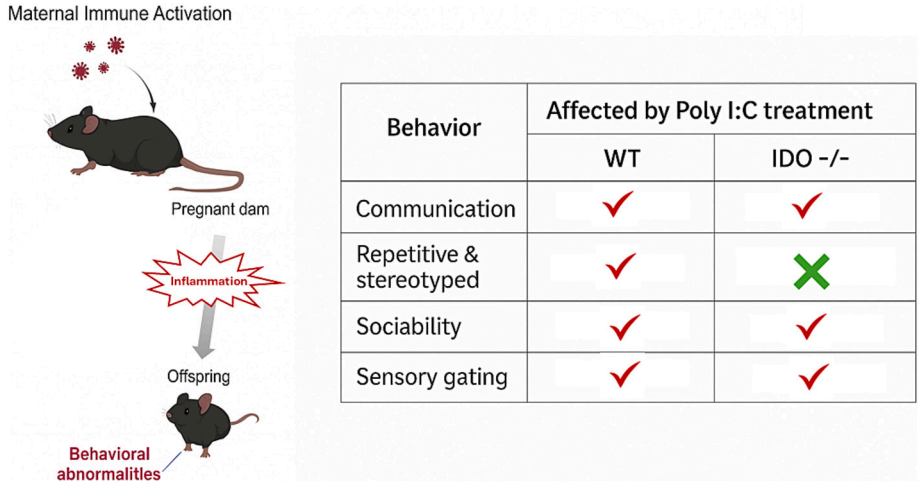

Fig. 10. Schematic illustrating the selective behavioral protection of IDO−/− mice. Wild-type offspring of Poly IC treated dams exhibited deficits in communication, increased repetitive and stereotyped behavior, deficits in sociability and sensory gating. Notably, IDO −/− of MIA dams developed similar phenotypes with the exception of increased repetitive and stereotyped behaviors.

been developed over the past several decades, including bacterial, viral, parasitic, and experimental models. In our study, we utilized the mouse poly IC model developed and validated in the early 2000s by Paul Patterson's research group (Garay et al., 2013; Smith et al., 2007a). Poly IC is a synthetic analog of double-stranded RNA that acts as a Toll-like receptor 3 agonist and viral mimetic. When administered prenatally, poly IC causes behavioral phenotypes to appear in the offspring after birth. While the specific time during gestation when the maternal immune challenge occurs seems to be important in determining the precise behavioral phenotypes that emerge, poly IC administration at GD 12.5

results in behavioral changes reminiscent of autism spectrum disorder, including repetitive and stereotyped behavior, deficits in sociability and communication. The poly IC model has been validated in both rodents and non-human primate models (Bauman et al., 2014; Estes et al., 2020; Santana-Coelho et al., 2021). Our data are entirely consistent with previous data in this regard, with reduced vocalization, increased repetitive/stereotyped behavior, reduced social preference, and apparent deficits in sensorimotor gating. In addition to confirming these previous findings, we further characterized the nature of communication deficits in a manner that has not previously been reported in this model using IDO knockout mice. Specifically, using DeepSqueak, a deep learning software that detects and analyzes vocalizations, we were able to not just build a repertoire for each of the groups in our study, but also identify differences in several parameters. Call length, main frequency, frequency distribution, interval between calls, distribution of the calls during the recording, and several other features of vocalizations were identified by DeepSqueak. Here, we demonstrate the effect of MIA across several vocalization features, including the complexity of the repertoire and the usage of specific calls by each group. Our analysis revealed that the effect of MIA on isolation-induced vocalizations in one-week old pups is similar in WT and in IDO−/−. Further investigation across a more comprehensive developmental timeline using DeepSqueak to analyze communication patterns in adolescent, young adult, and adult mice exposed to maternal immune activation would be interesting and important in follow-up studies.

The mechanism by which MIA causes neurodevelopmental and behavioral disruption in the offspring has been the subject of intense interest. A series of studies by Paul Patterson's research group identified the cytokine IL-6 as a critical mediator of the effects of poly IC on the offspring. In fact, their research demonstrated, using genetic and pharmacological approaches (IL-6 knockouts, IL-6 neutralizing antibodies), that inhibition of IL-6 signaling in both maternal and fetal compartments prevents deficits in prepulse inhibition, sociability, and marble burying behavior in mice (Hsiao and Patterson, 2011; Smith et al., 2007a; Wu et al., 2017). Consistent with these previous studies, we observed an increase in placental IL-6 expression. Here, in the present study, we aimed to investigate the role of the kynurenine pathway in the pathogenic mechanism of prenatal poly IC, downstream of IL-6 signaling.

We and others have previously demonstrated the important mechanistic role of IDO in mediating the neuroinflammatory effects of immune activation in adult mice (Hoshi et al., 2014; Lawson et al., 2013; O'Connor et al., 2009), and proinflammatory cytokines, including IL-6, can upregulate IDO and KP metabolism. In addition, prenatal and neonatal exposure to increased levels of kynurenine induces deficits in prepulse inhibition, memory, and social behavior (Iaccarino et al., 2013; Liu et al., 2014b; Pocivavsek et al., 2014). Therefore, to directly test whether IDO plays an important pathogenic role in poly IC-induced ASD-like behaviors, we utilized mice with targeted deletion of the IDO1 gene. IDO−/− offspring of dams treated with poly IC exhibited deficits in communication and social behavior. However, IDO1 deletion was protective against the development of repetitive and stereotyped behavior measured in the self-grooming test and the marble burying test. Taken together, these data indicate that IDO1-mediated KP metabolism plays an important mechanistic role in a subset of the behavioral consequences of MIA. While not directly investigated in the present study, these data may indicate that discrete brain regions or neural circuits responsible for regulating the development of repetitive/stereotyped behaviors are uniquely sensitive to changes in KP metabolism during what is roughly equivalent to the late first trimester/ early second trimester. Our data may provide a path toward identifying discrete circuitry underlying these behaviors that could be applicable in other disease contexts such as obsessive-compulsive disorder and anxiety.

To better understand the effect of deleting the rate-limiting and cytokine-inducible KP enzyme IDO1 in the development of offspring, we assessed whether the IDO−/− immune response to the poly IC challenge was different than WT mice. IDO has long been recognized to exert play important immunomodulatory effects in the context of immune tolerance, tumorigenesis, and sepsis, but it remains unclear whether IDO1 plays a role in regulating acute inflammation, particularly during gestation. In maternal plasma, 24 h after poly IC administration, we did not measure a significant increase in IL-6 as we expected, but there was a significant increase in the chemokine monocyte chemoattractant protein 1 (MCP-1) and the TLR3 inducible target interferon gamma-induced protein 10 (IP-10) in WT dams. It may be the case that the IL-6 response occurred before 24 h in our study. Interestingly, in IDO−/− dams, there was no increase in MCP-1 after poly IC, but the upregulation of IP-10 levels was comparable to WT mice. IP-10 is known to be induced by IFN-gamma or activation of TLR3 signaling, which is triggered by poly IC. Similar upregulation of IP-10 in both WT and IDO −/− mice indicates that the TLR3-mediated immune response to poly IC is robust in both genotypes. However, it is not immediately clear why MCP-1 levels are only upregulated in WT mice. It is possible that MCP-1 expression is regulated by KP metabolites through a yet to be described mechanism, or it is possible that the cross-sectional nature of our study was unable to capture genotype effects on the temporal expression pattern of poly IC inducible targets. There is some evidence in the literature consistent with our observation suggesting a role for IDO in the expression of MCP-1. Smith et al. showed that IDO1 deficiency attenuated the induction of MCP-1 in a study modeling KRAS-induced lung carcinoma. In the study, the authors used a cre-expressing adenovirus vector administered to the animals to activate the latent oncogene $Kras^{G12D}$. In response to the activation of Kras, WT mice exhibit increased levels of MCP-1, while IDO1 −/− mice did not (C. Smith et al., 2012). However, the mechanism by which this occurs was not clarified. Additionally, neutralization of MCP-1 is protective against immune-mediated insults, such as allergic inflammation and endotoxin-induced diaphragmatic inflammation, by decreasing the production of inflammatory mediators such as cytokines and prostaglandins (Gonzalo et al., 1998; Labbe et al., 2010). The mechanism by which this protective effect happens is not understood, but since the same effect was not observed in the placenta at gestational day 13.5, an intact adult immune system appears to be necessary. In placental samples, the prenatal administration of poly IC had the same effects in both genotypes, an immune response characterized by increased levels of IL-6 and IP-10, suggesting that the placenta may be responding directly to poly IC rather than maternally-derived poly IC-induced cytokines.

The next step in our study was to assess how MIA affected kynurenine pathway metabolism in both maternal and fetal compartments. In pregnant dams, poly IC did not result in a significant change maternal circulating kynurenine levels. The only differences observed were decreased kynurenine levels in IDO−/−, which was expected since the rate-limiting enzyme in the pathway is lacking in these animals. In the placenta, we hypothesized that IDO1 would be upregulated following the administration of poly IC to the pregnant dams as previously described by Goeden et al. (Goeden et al., 2016a). However, 24 h after poly IC administration, there was no upregulation of IDO in the placenta. We cannot rule out the possibility that IDO expression simply peaks earlier and returns to baseline by 24 h in this model. André et al. (2008) demonstrated that IDO expression peaked 6 h in the hippocampus and hypothalamus of adult mice after peripheral immune challenge with LPS (André et al., 2008). The placenta is also considered a high IDO expressing tissue which may limit the enzymes's inducibility. Interestingly, the enzymes that we found to be upregulated following poly IC were KAT2 and HAAO. In the study by Goeden et al., poly IC was administered at a dose of 2 mg/kg in CD1 pregnant mice at gestational day 12. They observed increased expression of IDO up to 48 h after poly IC which differs from our results (Goeden et al., 2016b). However, we used a different dose of poly IC in our study (20 mg/kg) and a different mouse strain background (C57BL6/J). Several other factors could account for the differences in IDO upregulation between our studies, including basal maternal immune profile, poly IC lot, and animal housing (Kentner et al., 2018; Mueller et al., 2018; Schwartzer et al.,

2013b).

Regarding kynurenine metabolites, placental homogenates from WT MIA offspring contained increased levels of kynurenic acid, xanthurenic acid, and quinolinic acid that didn't reach statistical significance. These data suggest that in placental tissues, 24 h after poly IC, there is likely a global upregulation of the kynurenine pathway in WT mice at an earlier timepoint than the one which we measured the metabolites. IDO−/− mice were protected against this upregulation of the kynurenine pathway since they did not show trends toward increased metabolite level. Interestingly, while not directly tested, correlation analysis in the placenta revealed that IL-6 levels were positively correlated with placental kynurenine levels, suggesting local IL-6 expression could be driving the increase in IDO-dependent KP metabolism. Additional experiments outside the scope of this manuscript will be required to explore this more fully. As expected, the correlation was not observed in IDO −/− mice. These data suggest that in the placental tissues, IL-6 can upregulate the KP by increasing the levels of kynurenine in WT mice, but in IDO−/− mice, IL-6 is unable to effect KP metabolism via IDO-1 expression.

As the placenta is an important source of nutrients and neurotransmitters to the developing fetal brain, we also measured KP metabolites in whole fetal brain homogenates 24 h after the poly IC challenge. MIA increased the levels of kynurenine and quinolinic acid in both genotypes, suggesting that the enzymes TDO and IDO2 could be responding to MIA-related signals locally. Additionally, there was an increase in KYNA levels only in WT brains that failed to reach statistical significance. Previous studies directly manipulating kynurenine and kynurenic acid levels reveal that experimentally increasing KYNA concentrations in the fetal brain during gestation results in behavioral phenotypes similar to those observed in our study (Erhardt et al., 2016; Notarangelo & Pocivavsek, 2017b; Pocivavsek et al., 2014). A recent study showed that MIA through IL17A signaling induction at GD12.5 can significantly increase the levels of KP metabolites in the fetal brain and placenta days after MIA (GD18.5). These findings corroborate with our study and also suggest that the alterations in the KP might take longer than 24 h to be fully established (Murakami et al., 2021).

Tryptophan is metabolized not only by the kynurenine pathway, but also through the serotonin metabolic pathway. Previous studies have shown that serotonin may be involved in the effects the response of the maternal/fetal tissues to infection. Goeden and collaborators reported no increased in 5-HT and 5-HIAA 24 h after poly IC in the fetal brain and placenta. This study, however, showed an increase in 5-HT in the forebrain 48 h after treatment. Another interesting finding from this study was that the conversion of tryptophan to serotonin also increased in the placenta 48 h in vitro (Goeden et al., 2016a). MIA, with the same protocol used in our study, has previously been shown to increase the levels of the 5-HT transporter in the hippocampus of adult mice (Reisinger et al., 2016). Another study, using LPS, showed that the immune stimulus alters expression of tryptophan hydroxylase (tph) 1 and 2 throughout development until adulthood in the brain of mice (Hsueh et al., 2017). Together, these studies demonstrated that immune stimulus could alter serotonergic metabolism. Hence, we decided to assess if there were alterations in the levels of 5-HT and its metabolite 5-HIAA in the maternal plasma, placenta, and fetal brain 24 h after poly IC administration to the dams. Our study showed no effects of MIA on 5-HT and 5-HIAA levels in the samples at the timepoint in which we collected our samples. The only effect we identified was that 5-HT was decreased in IDO−/− placentas when compared to WT placentas. Based on the findings of Goeden et al. (2016a), we can hypothesize that the reason we did not find any effects of Poly IC was because 24 h is too early to see an increase in 5-HT levels. The main findings of the Goeden study regarding 5-HT occurred 48 h after treatment. Thus, a later timepoint collection might be necessary to identify any significant alteration in 5-HT metabolism.

Research has demonstrated the potential role of decreased NMDA receptor expression and/or signaling in autism and schizophrenia. Gandal et al. reported that NR1 knockouts, mice that have reduced expression of the obligatory NMDA receptor subunit NR1, exhibit all core features of autism (Gandal et al., 2012). Thus, we also measured the expression of NMDA receptor subunits in our study to assess wether the regulation of glutamatergic neurotransmission could be associated with the protective effect observed in IDO−/− mice. Our results revealed that prenatal inflammation decreased the expression of NR1 and NR2B subunits in WT fetal brain 24 h after poly IC. Interestingly, IDO −/− did not have any modulatory effect on NMDA receptor subunits in response to MIA. A potential caveat in our study is that IDO−/− present, at baseline, decreased expression of NMDAr subunits when compared to control WT. This differential NMDAr expression profile could be the reason why these animals do not show any effect of poly IC at brain expression levels. Nonetheless, IDO−/− mice are protected against MIA-induced downregulation of NMDAr subunits at the timepoint that we measured, and this phenomenon could be associated with the lack of disruption of repetitive/stereotyped behavior in IDO−/− mice. Alternatively, it is possible that the temporal expression pattern of NMDA receptors in IDO−/− fetal brain simply occurs differently than in WT brains, which could explain why they do not exhibit an effect of poly IC in our study. Furthermore, studies have shown that prenatal administration of kynurenine induces increased brain levels of KYNA accompanied by decreased expression of NMDAr subunits (Pershing et al., 2016), which is consistent with the data we report here.

5. Limitations

It is important to note that only male offspring were assessed in this study, which is a limitation that will need to be addressed in future studies along with investigating the precise relationship between IDO −/− genotype and NMDA receptor expression. Even though ASD is more prevalent in males and the placental responses to prenatal immune challenge vary by sex, contemporary thought has begun to consider the notion that ASD presents differently between sexes providing another important reason to warrant systematic investigation of IDO x MIA interactions in female offspring.

6. Conclusion

Together, our findings reveal that the kynurenine pathway plays a pathogenic role in the development of repetitive/stereotyped behavior induced by maternal immune activation. Our data suggest that placental IL-6 likely upregulates KP metabolism resulting in increased exposure of the fetal brain to downstream metabolites such as QUIN and KYNA. Considering that these metabolites are modulators of NMDAr, it is plausible that prenatal inflammation, through upregulation of the KP pathway metabolism, disrupts the glutamatergic system leading to behavioral phenotypes. It is important to note, however, that our study was performed only on male offspring, and it is known that inflammation can cause dimorphic responses. Hence, it is necessary that future studies evaluate if our findings can be replicated in female offspring.

Ethics approval and consent

Research was approved by Institutional Animal Care and Use Committee at the University of Texas Health Science Center at San Antonio.

Author's contribution

D.S·C carried out experiments, collected and analyzed data, prepared the manuscript. R.S·B and R.N.R. analyzed USV data. M.A.F consulted on statistical analysis/reporting, generated the heat map, prepared the graphical abstract, reviewed and edited the final revised manuscript. J. O.C. conceptualized the study, coordinated research team, oversaw data collection and analysis, and prepared final manuscript.

CRediT authorship contribution statement

Danielle Santana-Coelho: Writing – review & editing, Writing – original draft, Funding acquisition, Formal analysis, Data curation. **Rafael dos Santos de Bessa:** Writing – original draft, Formal analysis. **Rodrigo Neves Romcy-Pereira:** Formal analysis. **Miguel A. de la Flor:** Writing – review & editing, Visualization, Software, Data curation, Conceptualization. **Jason C. O'Connor:** Writing – review & editing, Writing – original draft, Visualization, Supervision, Resources, Project administration, Methodology, Funding acquisition, Formal analysis, Conceptualization.

Consent for publication

Not applicable.

Funding

This work was supported by the National Institute of Health (R01 MH090127) and Morrison Trust. DSC was supported by the Coordenação de Aperfeiçoamento de Pessoal de Nível Superior – Brasil (CAPES) (Finance Code 001) and T32 HL007446.

Declaration of competing interest

The authors declare they have no competing interests.

Acknowledgements

We would like to thank Laney Redus for her contribution to collecting data for me manuscript.

Appendix A. Supplementary data

Supplementary data to this article can be found online at https://doi.org/10.1016/j.nbd.2026.107282.

Data availability

All data generated and analyzed during this study will be made available by the authors, without undue reservation.

References

André, C., O'Connor, J.C., Kelley, K.W., Lestage, J., Dantzer, R., Castanon, N., 2008. Spatio-temporal differences in the profile of murine brain expression of proinflammatory cytokines and indoleamine 2,3-dioxygenase in response to peripheral lipopolysaccharide administration. J. Neuroimmunol. 200 (1–2), 90–99. https://doi.org/10.1016/j.jneuroim.2008.06.011.

Atladóttir, H.Ó., Thorsen, P., Østergaard, L., Schendel, D.E., Lemcke, S., Abdallah, M., Parner, E.T., 2010a. Maternal infection requiring hospitalization during pregnancy and autism spectrum disorders. J. Autism Dev. Disord. 40 (12), 1423–1430. https://doi.org/10.1007/s10803-010-1006-y.

Atladóttir, H.Ó., Thorsen, P., Schendel, D.E., Østergaard, L., Lemcke, S., Parner, E.T., 2010b. Association of hospitalization for infection in childhood with diagnosis of autism spectrum disorders: a Danish cohort study. Arch. Pediatr. Adolesc. Med. 164 (5), 470–477. https://doi.org/10.1001/archpediatrics.2010.9.

Bauman, M.D., Iosif, A.-M., Smith, S.E.P., Bregere, C., Amaral, D.G., Patterson, P.H., 2014. Activation of the maternal immune system during pregnancy alters behavioral development of Rhesus monkey offspring. Biol. Psychiatry 75 (4), 332–341. https://doi.org/10.1016/j.biopsych.2013.06.025.

Beversdorf, D.Q., Stevens, H.E., Jones, K.L., 2018. Prenatal stress, maternal immune dysregulation, and their association with autism spectrum disorders. Curr. Psychiatry Rep. 20 (9), 1–12. Current Medicine Group LLC 1. https://doi.org/10.1007/s11920-018-0945-4.

Bolton, J.L., Auten, R.L., Bilbo, S.D., 2014. Prenatal air pollution exposure induces sexually dimorphic fetal programming of metabolic and neuroinflammatory outcomes in adult offspring. Brain Behav. Immun. 37, 30–44. https://doi.org/10.1016/j.bbi.2013.10.029.

Boulanger-Bertolus, J., Pancaro, C., Mashour, G.A., 2018. Increasing role of maternal immune activation in neurodevelopmental disorders. Front. Behav. Neurosci. 12. https://doi.org/10.3389/fnbeh.2018.00230.

Campbell, B.M., Charych, E., Lee, A.W., Möller, T., 2014. Kynurenines in CNS disease: regulation by inflammatory cytokines. Front. Neurosci. 8, 12. https://doi.org/10.3389/fnins.2014.00012.

Center for Disease Control and Prevention, 2025. Data and Statistics on Autism Spectrum Disorder. https://www.cdc.gov/autism/data-research/index.html.

Christensen, J., Grønborg, T.K., Sørensen, M.J., Schendel, D., Parner, E.T., Pedersen, L.H., Vestergaard, M., 2013. Prenatal valproate exposure and risk of autism spectrum disorders and childhood autism. JAMA 309 (16), 1696–1703. https://doi.org/10.1001/jama.2013.2270.

Coffey, K.R., Marx, R.G., Neumaier, J.F., 2019. DeepSqueak: a deep learning-based system for detection and analysis of ultrasonic vocalizations. Neuropsychopharmacology 44 (5), 859–868. https://doi.org/10.1038/s41386-018-0303-6.

Dahlgren, J., Samuelsson, A.M., Jansson, T., Holmäng, A., 2006. Interleukin-6 in the maternal circulation reaches the rat fetus in mid-gestation. Pediatr. Res. 60 (2), 147–151. https://doi.org/10.1203/01.pdr.0000230026.74139.18.

Erhardt, S., Pocivavsek, A., Repici, M., Liu, X.-C., Imbeault, S., Maddison, D.C., Thomas, M.A.R., Smalley, J.L., Larsson, M.K., Muchowski, P.J., Giorgini, F., Schwarcz, R., 2016. Adaptive and behavioral changes in kynurenine 3-monooxygenase knockout mice: relevance to psychotic disorders. Biol. Psychiatry. https://doi.org/10.1016/j.biopsych.2016.12.011.

Estes, M.L., Prendergast, K., MacMahon, J.A., Cameron, S., Paul Aboubechara, J., Farrelly, K., Sell, G.L., Haapanen, L., Schauer, J.D., Horta, A., Shaffer, I.C., Le, C.T., Kincheloe, G.N., Tan, D.J., van der List, D., Bauman, M.D., Carter, C.S., Van de Water, J., McAllister, A.K., 2020. Baseline immunoreactivity before pregnancy and poly(I:C) dose combine to dictate susceptibility and resilience of offspring to maternal immune activation. Brain Behav. Immun. 88, 619–630. https://doi.org/10.1016/j.bbi.2020.04.061.

Gandal, M.J., Anderson, R.L., Billingslea, E.N., Carlson, G.C., Roberts, T.P.L., Siegel, S.J., 2012. Mice with reduced NMDA receptor expression: more consistent with autism than schizophrenia? Genes Brain Behav. 11 (6). https://doi.org/10.1111/j.1601-183X.2012.00816.x.

Garay, P.A., Hsiao, E.Y., Patterson, P.H., Mcallister, A.K., 2013. Maternal Immune Activation Causes Age- and Region-Specific Changes in Brain Cytokines in Offspring Throughout Development. https://doi.org/10.1016/j.bbi.2012.07.008.

Goeden, N., Velasquez, J., Arnold, K.A., Chan, Y., Lund, B.T., Anderson, G.M., Bonnin, A., 2016. Maternal inflammation disrupts fetal neurodevelopment via increased placental output of serotonin to the fetal brain. J. Neurosci. https://doi.org/10.1523/JNEUROSCI.2534-15.2016.

Gonzalo, J.A., Lloyd, C.M., Wen, D., Albar, J.P., Wells, T.N.C., Proudfoot, A., Martinez-A, C., Dorf, M., Bjerke, T., Coyle, A.J., Gutierrez-Ramos, J.C., 1998. The coordinated action of CC chemokines in the lung orchestrates allergic inflammation and airway hyperresponsiveness. J. Exp. Med. 188 (1), 157–167. https://doi.org/10.1084/jem.188.1.157.

Heisler, J.M., O'Connor, J.C., 2015. Indoleamine 2,3-dioxygenase-dependent neurotoxic kynurenine metabolism mediates inflammation-induced deficit in recognition memory. Brain Behav. Immun. 50, 115–124. https://doi.org/10.1016/j.bbi.2015.06.022.

Hoshi, M., Osawa, Y., Ito, H., Ohtaki, H., Ando, T., Takamatsu, M., Hara, A., Saito, K., Seishima, M., 2014. Blockade of indoleamine 2,3-dioxygenase reduces mortality from peritonitis and sepsis in mice by regulating functions of CD11b+ peritoneal cells. Infect. Immun. 82 (11), 4487–4495. https://doi.org/10.1128/IAI.02113-14.

Hsiao, E.Y., Patterson, P.H., 2011. Activation of the maternal immune system induces endocrine changes in the placenta via IL-6. Brain Behav. Immun. 25 (4), 604–615. https://doi.org/10.1016/j.bbi.2010.12.017.

Hsueh, P.-T., Wang, H.-H., Liu, C.-L., Ni, W.-F., Chen, Y.-L., Liu, J.-K., 2017. Expression of cerebral serotonin related to anxiety-like behaviors in C57BL/6 offspring induced by repeated subcutaneous prenatal exposure to low-dose lipopolysaccharide. PLoS One 12 (6), e0179970. https://doi.org/10.1371/journal.pone.0179970.

Iaccarino, H.F., Suckow, R.F., Xie, S., Bucci, D.J., 2013. The effect of transient increases in kynurenic acid and quinolinic acid levels early in life on behavior in adulthood: implications for schizophrenia. Schizophr. Res. 150 (2–3). https://doi.org/10.1016/j.schres.2013.09.004.

Kegel, M.E., Bhat, M., Skogh, E., Samuelsson, M., Lundberg, K., Dahl, M.L., Sellgren, C., Schwieler, L., Engberg, G., Schuppe-Koistinen, I., Erhardt, S., 2014. Imbalanced kynurenine pathway in schizophrenia. Int. J. Tryptophan Res. 7, 15–22. https://doi.org/10.4137/IJTR.S16800.

Kentner, A.C., Bilbo, S.D., Brown, A.S., Hsiao, E.Y., McAllister, A.K., Meyer, U., Pearce, B. D., Pletnikov, M.V., Yolken, R.H., Bauman, M.D., 2018. Maternal immune activation: reporting guidelines to improve the rigor, reproducibility, and transparency of the model. Neuropsychopharmacology 1. https://doi.org/10.1038/s41386-018-0185-7.

Kindler, J., Lim, C.K., Weickert, C.S., Boerrigter, D., Galletly, C., Liu, D., Jacobs, K.R., Balzan, R., Bruggemann, J., O'Donnell, M., Lenroot, R., Guillemin, G.J., Weickert, T. W., 2019. Dysregulation of kynurenine metabolism is related to proinflammatory cytokines, attention, and prefrontal cortex volume in schizophrenia. Mol. Psychiatry 1–13. https://doi.org/10.1038/s41380-019-0401-9.

Labbe, K., Danialou, G., Gvozdic, D., Demoule, A., Divangahi, M., Boyd, J.H., Petrof, B.J., 2010. Inhibition of monocyte chemoattractant protein-1 prevents diaphragmatic inflammation and maintains contractile function during endotoxemia. Crit. Care 14 (5), R187. https://doi.org/10.1186/cc9295.

Lawson, M.A., Parrott, J.M., McCusker, R.H., Dantzer, R., Kelley, K.W., O'Connor, J.C., 2013. Intracerebroventricular administration of lipopolysaccharide induces indoleamine-2,3-dioxygenase-dependent depression-like behaviors. J. Neuroinflammation 10, 87. https://doi.org/10.1186/1742-2094-10-87.

Lehmann, J., Schaefer, P., Ferkany, J.W., Coyle, J.T., 1983. Quinolinic acid evokes [3H] acetylcholine release in striatal slices: mediation by NMDA-type excitatory amino

acid receptors. Eur. J. Pharmacol. 96 (1–2), 111–115. https://doi.org/10.1016/0014-2999(83)90536-8.
Lim, C.K., Essa, M.M., de Paula Martins, R., Lovejoy, D.B., Bilgin, A.A., Waly, M.I., Al-Farsi, Y.M., Al-Sharbati, M., Al-Shaffae, M.A., Guillemin, G.J., 2016. Altered kynurenine pathway metabolism in autism: implication for immune-induced glutamatergic activity. Autism Res. 9 (6), 621–631. https://doi.org/10.1002/aur.1565.
Liu, X.-C., Holtze, M., Powell, S.B., Terrando, N., Larsson, M.K., Persson, A., Olsson, S.K., Orhan, F., Kegel, M., Asp, L., Goiny, M., Schwieler, L., Engberg, G., Karlsson, H., Erhardt, S., 2014. Behavioral disturbances in adult mice following neonatal virus infection or kynurenine treatment – role of brain kynurenic acid. Brain Behav. Immun. 36, 80–89. https://doi.org/10.1016/j.bbi.2013.10.010.
Malkova, N.V., Yu, C.Z., Hsiao, E.Y., Moore, M.J., Patterson, P.H., 2012. Maternal immune activation yields offspring displaying mouse versions of the three core symptoms of autism. Brain Behav. Immun. 26 (4), 607–616. https://doi.org/10.1016/J.BBI.2012.01.011.
McTighe, S.M., Neal, S.J., Lin, Q., Hughes, Z.A., Smith, D.G., 2013. The BTBR mouse model of autism spectrum disorders has learning and attentional impairments and alterations in acetylcholine and kynurenic acid in prefrontal cortex. PLoS One 8 (4). https://doi.org/10.1371/journal.pone.0062189.
Meehan, C., Harms, L., Frost, J.D., Barreto, R., Todd, J., Schall, U., Shannon Weickert, C., Zavitsanou, K., Michie, P.T., Hodgson, D.M., 2017. Effects of immune activation during early or late gestation on schizophrenia-related behaviour in adult rat offspring. Brain Behav. Immun. 63, 8–20. https://doi.org/10.1016/J.BBI.2016.07.144.
Mosienko, V., Beis, D., Alenina, N., Wöhr, M., 2015. Reduced isolation-induced pup ultrasonic communication in mouse pups lacking brain serotonin. Mol. Autism 6 (1). https://doi.org/10.1186/s13229-015-0003-6.
Mueller, F.S., Polesel, M., Richetto, J., Meyer, U., Weber-Stadlbauer, U., 2018. Mouse models of maternal immune activation: mind your caging system! Brain Behav. Immun. 73, 643–660. https://doi.org/10.1016/J.BBI.2018.07.014.
Murakami, Y., Imamura, Y., Kasahara, Y., Yoshida, C., Momono, Y., Fang, K., Nishiyama, T., Sakai, D., Konishi, Y., 2021. The effects of maternal interleukin-17A on social behavior, cognitive function, and depression-like behavior in mice with altered kynurenine metabolites. Int. J. Tryptophan Res. 14. https://doi.org/10.1177/11786469211026639.
Notarangelo, F.M., Pocivavsek, A., 2017. Elevated kynurenine pathway metabolism during neurodevelopment: implications for brain and behavior. Neuropharmacology 112, 275–285. Elsevier Ltd. https://doi.org/10.1016/j.neuropharm.2016.03.001.
O'Connor, J.C., Lawson, M.A., André, C., Briley, E.M., Szegedi, S.S., Lestage, J., Castanon, N., Herkenham, M., Dantzer, R., Kelley, K.W., 2009. Induction of IDO by Bacille Calmette-Guérin is responsible for development of murine depressive-like behavior. J. Immunol. 182 (5), 3202–3212. https://doi.org/10.4049/jimmunol.0802722.
Parrott, J.M., Redus, L., Santana-Coelho, D., Morales, J., Gao, X., O'Connor, J.C., 2016. Neurotoxic kynurenine metabolism is increased in the dorsal hippocampus and drives distinct depressive behaviors during inflammation. Transl. Psychiatry 6 (10). https://doi.org/10.1038/tp.2016.200.
Perez, S.M., Donegan, J.J., Lodge, D.J., 2019. Effect of estrous cycle on schizophrenia-like behaviors in MAM exposed rats. Behav. Brain Res. 362, 258–265. https://doi.org/10.1016/J.BBR.2019.01.031.
Perkins, M.N., Stone, T.W., 1982. An iontophoretic investigation of the actions of convulsant kynurenines and their interaction with the endogenous excitant quinolinic acid. Brain Res. 247 (1), 184–187. https://doi.org/10.1016/0006-8993(82)91048-4.
Pershing, M.L., Phenis, D., Valentini, V., Pocivavsek, A., Lindquist, D.H., Schwarcz, R., Bruno, J.P., 2016. Prenatal kynurenine exposure in rats: age-dependent changes in NMDA receptor expression and conditioned fear responding. Psychopharmacology 233 (21−22), 3725–3735. https://doi.org/10.1007/s00213-016-4404-9.
Pocivavsek, A., Thomas, M.A.R., Elmer, G.I., Bruno, J.P., Schwarcz, R., 2014. Continuous kynurenine administration during the prenatal period, but not during adolescence, causes learning and memory deficits in adult rats. Psychopharmacology 231 (14), 2799–2809. https://doi.org/10.1007/s00213-014-3452-2.
Reisinger, S.N., Kong, E., Khan, D., Schulz, S., Ronovsky, M., Berger, S., Horvath, O., Cabatic, M., Berger, A., Pollak, D.D., 2016. Maternal immune activation epigenetically regulates hippocampal serotonin transporter levels. Neurobiol. Stress 4, 34–43. https://doi.org/10.1016/j.ynstr.2016.02.007.
Saito, S., Saito, S., 2001. Cytokine cross-talk between mother and the embryo/placenta. J. Reprod. Immunol. 52 (52), 15–33.
Salazar, A., Gonzalez-Rivera, B.L., Redus, L., Parrott, J.M., O'Connor, J.C., 2012. Indoleamine 2,3-dioxygenase mediates anhedonia and anxiety-like behaviors caused by peripheral lipopolysaccharide immune challenge. Horm. Behav. 62 (3), 202–209. NIH Public Access. https://doi.org/10.1016/j.yhbeh.2012.03.010.
Santana-Coelho, D., 2024. Does the kynurenine pathway play a pathogenic role in autism spectrum disorder? Brain Behav. Immun. Health 40, 100839. https://doi.org/10.1016/j.bbih.2024.100839.
Santana-Coelho, D., Layne-Colon, D., Valdespino, R., Ross, C.C., Tardif, S.D., O'Connor, J.C., 2021. Advancing autism research from mice to marmosets: behavioral development of offspring following prenatal maternal immune activation. Front. Psychol. 12, 1295. https://doi.org/10.3389/FPSYT.2021.705554/BIBTEX.
Schmittgen, T.D., Livak, K.J., 2008. Analyzing real-time PCR data by the comparative CT method. Nat. Protoc. 3 (6), 1101–1108. https://doi.org/10.1038/nprot.2008.73.
Schwartzer, J.J., Careaga, M., Onore, C.E., Rushakoff, J.A., Berman, R.F., Ashwood, P., 2013. Maternal immune activation and strain specific interactions in the development of autism-like behaviors in mice. Transl. Psychiatry 3 (3), e240. https://doi.org/10.1038/tp.2013.16.
Smith, S.E.P., Li, J., Garbett, K., Mirnics, K., Patterson, P.H., 2007. Maternal immune activation alters fetal brain development through interleukin-6. J. Neurosci. 27 (40), 10695–10702. https://doi.org/10.1523/JNEUROSCI.2178-07.2007.
Smith, C., Chang, M.Y., Parker, K.H., Beury, D.W., DuHadaway, J.B., Flick, H.E., Boulden, J., Sutanto-Ward, E., Soler, A.P., Laury-Kleintop, L.D., Mandik-Nayak, L., Metz, R., Ostrand-Rosenberg, S., Prendergast, G.C., Muller, A.J., 2012. IDO is a nodal pathogenic driver of lung cancer and metastasis development. Cancer Discov. 2 (8), 722–735. https://doi.org/10.1158/2159-8290.CD-12-0014.
Vuillermot, S., Luan, W., Meyer, U., Eyles, D., 2017. Vitamin D treatment during pregnancy prevents autism-related phenotypes in a mouse model of maternal immune activation. Mol. Autism. 8 (1), 9. https://doi.org/10.1186/s13229-017-0125-0.
Wu, W.-L., Hsiao, E.Y., Yan, Z., Mazmanian, S.K., Patterson, P.H., 2017. The placental interleukin-6 signaling controls fetal brain development and behavior. Brain Behav. Immun. 62, 11–23. https://doi.org/10.1016/j.bbi.2016.11.007.